Inorganic Chemistry

Article

pubs.acs.org/IC

Synthesis and Hydride Transfer Reactions of Cobalt and Nickel Hydride Complexes to BX_3 Compounds

Michael T. Mock,* Robert G. Potter, Molly J. O'Hagan, Donald M. Camaioni, William G. Dougherty,† W. Scott Kassel,† and Daniel L. DuBois

Pacific Northwest National Laboratory, P.O. Box 999, Richland, Washington 99352, United States

†Department of Chemistry, Villanova University, Villanova, Pennsylvania 19085, United States

Supporting Information

ABSTRACT: Hydrides of numerous transition metal complexes can be generated by the heterolytic cleavage of H_2 gas such that they offer alternatives to using main group hydrides in the regeneration of ammonia borane, a compound that has been intensely studied for hydrogen storage applications. Previously, we reported that $HRh(dmpe)_2$ (dmpe = 1,2-bis(dimethylphosphinoethane)) was capable of reducing a variety of BX_3 compounds having a hydride affinity (HA) greater than or equal to the HA of BEt_3. This study examines the reactivity of less expensive cobalt and nickel hydride complexes, $HCo(dmpe)_2$ and $[HNi(dmpe)_2]^+$, to form B−H bonds. The hydride donor abilities ($\Delta G_{H^-}°$) of $HCo(dmpe)_2$ and $[HNi(dmpe)_2]^+$ were positioned on a previously established scale in acetonitrile that is cross-referenced with calculated HAs of BX_3 compounds. The collective data guided our selection of BX_3 compounds to investigate and aided our analysis of factors that determine favorability of hydride transfer. $HCo(dmpe)_2$ was observed to transfer H^- to BX_3 compounds with X = H, OC_6F_5, and SPh. The reaction with $B(SPh)_3$ is accompanied by the formation of dmpe-$(BH_3)_2$ and dmpe-$(BH_2(SPh))_2$ products that follow from a reduction of multiple B−SPh bonds and a loss of dmpe ligands from cobalt. Reactions between $HCo(dmpe)_2$ and $B(SPh)_3$ in the presence of triethylamine result in the formation of $Et_3N{-}BH_2SPh$ and $Et_3N{-}BH_3$ with no loss of a dmpe ligand. Reactions of the cationic complex $[HNi(dmpe)_2]^+$ with $B(SPh)_3$ under analogous conditions give $Et_3N{-}BH_2SPh$ as the final product along with the nickel−thiolate complex $[Ni(dmpe)_2(SPh)]^+$. The synthesis and characterization of $HCo(dedpe)_2$ (dedpe = $Et_2PCH_2CH_2PPh_2$) from H_2 and a base is also discussed, including the formation of an uncommon *trans* dihydride species, *trans*-$[(H)_2Co(dedpe)_2][BF_4]$.

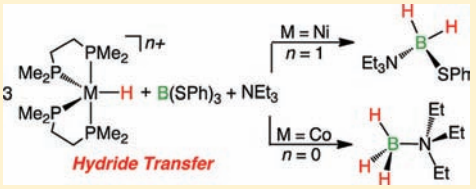

INTRODUCTION

Fundamental studies of dihydrogen binding to transition metal complexes have been examined in considerable detail.[1] Moreover, the use of H_2 to prepare transition-metal hydride complexes that are powerful hydride donors is of interest because it could provide an alternative to using traditional borohydride reagents that are generally expensive to produce and regenerate.[2] For example, methods to regenerate the chemical hydrogen storage material ammonia borane (AB, NH_3BH_3), a promising candidate for hydrogen storage[3] due to its gravimetric density of 19.6 wt % H_2, have used $LiAlH_4$, MgH_2, SnH, and N_2H_4 as a means to form B−H bonds.[4] Recently, as an alternative approach toward AB regeneration, we examined hydride transfer reactions between $HRh(dmpe)_2$ (dmpe = 1,2-bis(dimethylphosphinoethane)) and a series of BX_3 complexes (X = OR, SPh, F, H; R = Ph, *p*-C_6H_4OMe, C_6F_5, ^{t}Bu, $Si(Me)_3$) using a combination of experiment and theory.[5] Our goals were to provide a reliable and quantitative method for determining when hydride transfer from transition-metal hydrides to BX_3 compounds will be favorable. $HRh(dmpe)_2$ was chosen because it is one of the most powerful transition-metal hydride donors, and therefore hydride transfer reactions with a wide variety of BX_3 hydride acceptor compounds could be examined. Indeed, this study established that $HRh(dmpe)_2$ can effectively transfer a hydride ligand to BX_3 compounds, and in some cases multiple B−H bonds can be formed. These initial results proved favorable, however, in a practical system for AB regeneration, the use of transition metals much less expensive than rhodium will be required.

To address this requirement, we have taken advantage of previous studies regarding the structural and electronic factors that control the hydride donor ability of transition-metal hydride complexes with chelating diphosphine ligands, e.g., $HM(diphosphine)_2$ and $[HM'(diphosphine)_2]^+$ (M = Co or Rh and M′ = Ni, Pd, or Pt[6]). For strong hydride donors, the incorporation of electron-donating substituents on the diphosphine ligands[6,7] and a small natural bite angle[8] of the diphosphine are critical. Furthermore, the identity of the transition metal plays an important role, where second row transition metals have been shown to give better hydride donors than first and third row metals with identical diphosphine ligands.[9] Varying these structural and electronic parameters, hydride donor abilities can span a range of free energies associated with eq 1a ($\Delta G_{H^-}°$) from 26 to 76 kcal/mol,[5,10] with smaller values

Received: April 23, 2011
Published: October 31, 2011

of $\Delta G_{H^-}{}^{\circ}$ representing better hydride donors.

$$[HM(diphosphine)_2]^{n+} \rightarrow [M(diphosphine)_2]^{(n+1)+} + H^- \quad (1a)$$

Herein, we report the preparation, characterization, and hydride transfer reactions of first-row transition-metal hydride systems of cobalt and nickel, with the ultimate goal of developing catalytic processes based on these less expensive metals. In the current transition-metal hydride complexes of interest, i.e., $HCo(dmpe)_2$ and $[HNi(dmpe)_2]^+$, dmpe has been selected as the supporting diphosphine ligand due to the important structural and electronic considerations noted above. These transition-metal hydrides are evaluated for their ability to perform hydride transfer reactions with BX_3 compounds. BX_3 compounds are selected on the basis of their hydride acceptor ability and are proposed targets generated from the digestion of spent ammonia borane material.[11] Although a decrease in hydride donor ability according to eq 1a is expected in these systems compared to the $HRh(dmpe)_2$ system, our findings indicate that products containing multiple B−H bonds can be formed in these reactions. In addition to hydride transfer studies of $[HM(dmpe)_2]^{n+}$ (M = Co, Ni; n = 0, 1), we report the synthesis and characterization of $HCo(dedpe)_2$ (dedpe = $Et_2PCH_2CH_2PPh_2$) from H_2 and a base, highlighting interesting structural findings with the cobalt−dedpe complexes, and discuss initial hydride transfer chemistry.

RESULTS AND DISCUSSION

Synthesis and Characterization of $Co(dmpe)_2$ and $Co(dedpe)_2$ Complexes. Transition-metal hydrides have been prepared by a variety of synthetic routes. For example, $HCo(dppe)_2$ was prepared by reaction of an excess of a hydridic borohydride (e.g., $NaBH_4$) with $[Co(dppe)_2(CH_3CN)][BF_4]_2$ in ethanol.[12] Initially, we followed a similar procedure for the preparation of $HCo(dmpe)_2$. Although $HCo(dmpe)_2$ was produced, we found that this preparative route resulted in a variety of products resulting from undesirable side reactions such as the formation of dmpe−$(BH_3)_2$. $HCo(dmpe)_2$ was first reported by Schunn,[13] prepared from the reduction of $(dmpe)_2CoBr_2$ with sodium naphthalenide, followed by the addition of a stoichiometric amount of water or hydrogen gas. In the present work, we prepared $HCo(dmpe)_2$ from hydrogen using two separate synthetic routes. The first "one-pot" method, shown in reaction 1, is a modification of Schunn's procedure. $[Co(dmpe)_2(CH_3CN)_2][BF_4]_2$ is reduced with two equivalents of potassium graphite (KC_8) followed by exposure to hydrogen gas, affording $HCo(dmpe)_2$ in 60% yield. Using the second preparative method, reaction 2, two intermediate complexes are isolated on route to $HCo(dmpe)_2$. First, reduction of paramagnetic $[Co(dmpe)_2(CH_3CN)_2][BF_4]_2$ with one equivalent of KC_8 in acetonitrile produces the diamagnetic Co(I) species, $[Co(dmpe)_2(CH_3CN)][BF_4]$, in moderate yield. ^1H and ^{31}P NMR signals for all diamagnetic complexes reported in this study exhibit broadening due to the S = 7/2 spin of the ^{59}Co nucleus. In THF-d_8, $[Co(dmpe)_2(CH_3CN)][BF_4]$ exhibits a singlet at δ 50.7 in the ^{31}P NMR spectrum consistent with four magnetically equivalent phosphorus atoms. The addition of H_2 gas to a THF or acetonitrile solution of $[Co(dmpe)_2(CH_3CN)][BF_4]$ produces the six-coordinate dihydride, *cis*-$[(H)_2Co(dmpe)_2][BF_4]$. The ^{31}P NMR spectrum recorded in THF-d_8 contains two broad resonances at δ 61.2 and 51.6, a

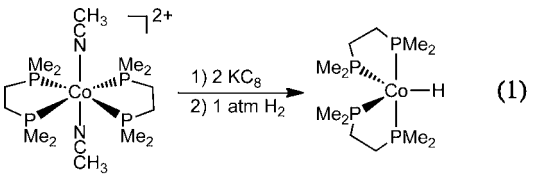

(1)

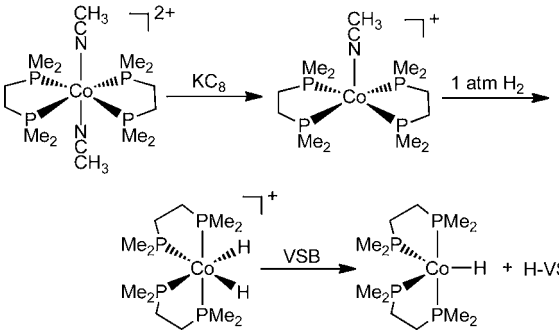

(2)

consequence of the asymmetry of the complex and coupling to the ^{59}Co nucleus. Additionally, the hydride ligands appear as a broad resonance at δ −14.5 in the ^1H NMR spectrum. The addition of Verkade's base ($P(CH_3NCH_2CH_2)_3N$, VSB; pK_a = 32.9 in acetonitrile[14]) to a THF solution of *cis*-$[(H)_2Co(dmpe)_2][BF_4]$ results in the precipitation of $[HP(CH_3NCH_2CH_2)_3N][BF_4]$ and concomitant formation of $HCo(dmpe)_2$. The ^{31}P NMR spectrum of this fluxional five-coordinate cobalt hydride contains a broad singlet centered at δ 46.6. The hydride resonance in the ^1H NMR spectrum is a quintet at δ −16.6.

An analogous three-step procedure, as shown in reaction 2, was used to prepare the cobalt complexes containing the asymmetric dedpe ligand. Starting from the paramagnetic cobalt(II) complex, $[Co(dedpe)_2(CH_3CN)][BF_4]_2$, the addition of one equivalent of KC_8 in acetonitrile affords the diamagnetic complex $[Co(dedpe)_2(CH_3CN)][BF_4]$. This complex is sensitive to solvent conditions. In acetonitrile, the solution is orange, corresponding to the five-coordinate square-pyramidal complex $[Co(dedpe)_2(CH_3CN)][BF_4]$ with acetonitrile bound in the axial position. Removal of acetonitrile under vacuum conditions results in a darkening of the solid. The addition of THF results in a drastic color change to dark blue due to a loss of the acetonitrile ligand, affording the 16-electron complex, $[Co(dedpe)_2][BF_4]$, confirmed by X-ray crystallography (discussed below). The ^{31}P NMR spectrum of $[Co(dedpe)_2(CH_3CN)][BF_4]$ in CD_3CN contains two resonances, a broad triplet at δ 68.8 ($^2J_{PP}$ = 63 Hz) and a very broad singlet (or more likely an unresolved triplet that is severely broadened by the cobalt quadrupole) at δ 62.8, due to the two chemically inequivalent phosphorus environments of the dedpe ligand. The exposure of a solution of $[Co(dedpe)_2(CH_3CN)][BF_4]$ to H_2 gas results in an immediate color change from orange to pale yellow, affording *cis* and *trans* isomers of the cobalt(III) dihydride complex $[(H)_2Co(dedpe)_2][BF_4]$ according to ^1H and ^{31}P NMR spectroscopic data. ^{31}P NMR spectra recorded at 25 °C exhibit remarkably broad, unresolved resonances between δ 67 and 90. Cooling the sample to −40 °C results in a significant improvement in resolution of the ^{31}P NMR resonances (Figure S5, Supporting Information). At this temperature, nine broad signals are observed. The inherent complexity of the ^{31}P NMR spectrum is attributed to the asymmetry of the dedpe ligand and the presence of multiple dihydride isomers in solution. Examination of the ^1H NMR

dx.doi.org/10.1021/ic200857x | Inorg. Chem. 2011, 50, 11914–11928

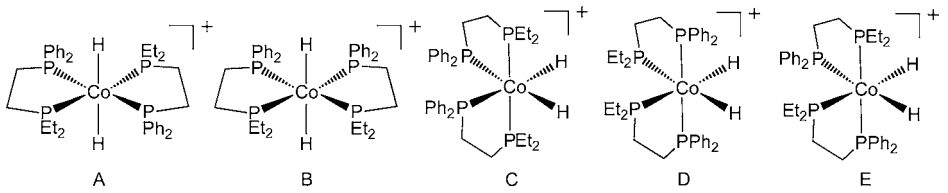

Figure 1. The structures of *trans*-dihydride (structures A and B) and *cis*-dihydride (structures C–E) isomers formed from the addition of H_2 to $[Co(dedpe)_2(CH_3CN)]^+$.

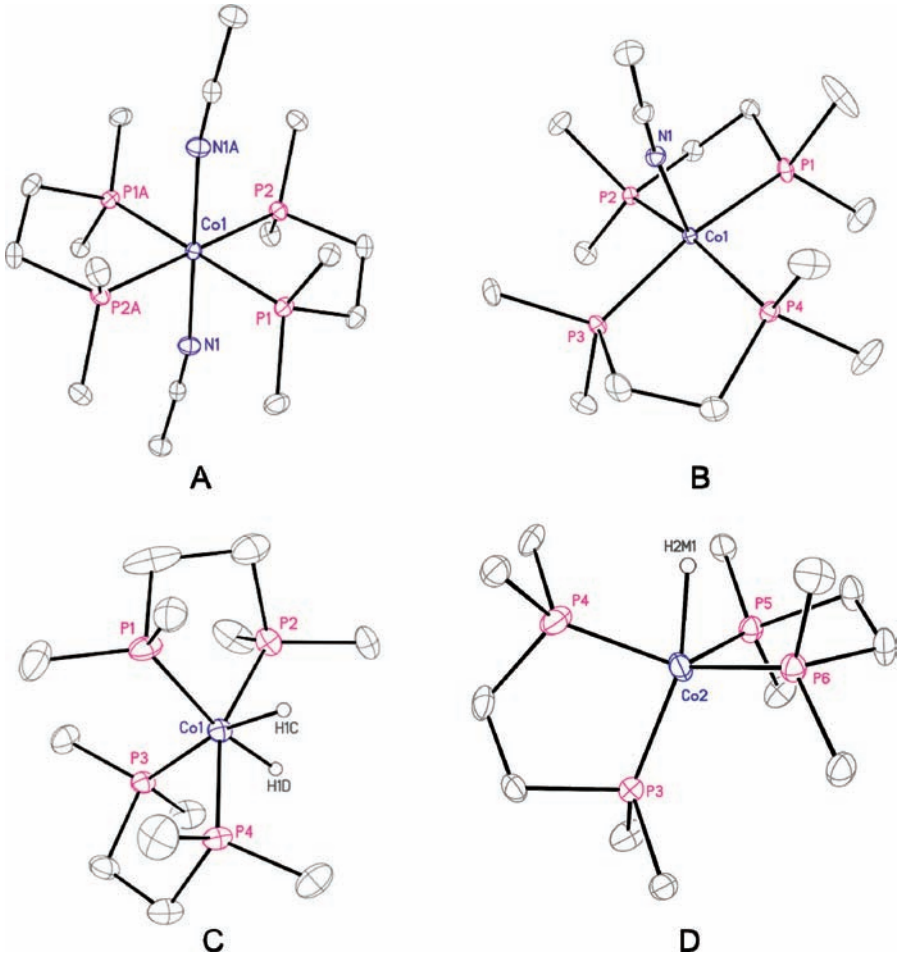

Figure 2. Molecular structures of (A) $[Co(dmpe)_2(CH_3CN)_2]^{2+}$, (B) $[Co(dmpe)_2(CH_3CN)]^+$, (C) *cis*-$[(H)_2Co(dmpe)_2]^+$, and (D) $HCo(dmpe)_2$ with atom numbering. Thermal ellipsoids drawn at 30% probability. Hydrogen atoms omitted except for hydride ligands attached to Co in structures C and D.

spectrum at 25 °C shows three broad, unresolved peaks in the hydride region around δ −14. Upon cooling the sample to −40 °C, four broad signals are present. The three broad features at δ −14 are assigned as *cis*-dihydride products, while the new quintet resonance at δ −10.9 is assigned as the *trans*-dihydride isomer (Figure S6, Supporting Information). In a recent report of *cis* and *trans* isomers of $Ir(H)_2(dppm)_2$, a similar downfield hydride resonance was observed for *trans*-$[Ir(H)_2(dppm)_2]$ at δ −7.6 compared to *cis*-$[Ir(H)_2(dppm)_2]$[15] at δ −11.4. In the present case, further examination of the hydride region in the $^1H\{^{31}P\}$ NMR spectrum displays a singlet for the *trans* isomer and four broad, overlapping resonances at δ −13.6, −13.7, −14.0, and −14.6 for the *cis*-dihydride isomers. The possible structures of *trans*- and *cis*-dihydride isomers for $[(H)_2Co(dedpe)_2]^+$ are shown in Figure 1.

The addition of Verkade's base to a THF solution of $[(H)_2Co(dedpe)_2][BF_4]$ affords a red solution of $HCo(dedpe)_2$ and the precipitation of the protonated base, $[HP(CH_3NCH_2CH_2)_3N][BF_4]$. The five-coordinate cobalt–hydride exhibits broad signals at δ 79.1 and 74.2 in the ^{31}P NMR spectrum and a quintet at δ −15.9 in the ^1H NMR spectrum corresponding to the hydride resonance.

Structural Studies. X-ray crytallographic studies were carried out for each synthetic step in the preparation of $HCo(dmpe)_2$ and $HCo(dedpe)_2$. Molecular structures of $[Co(dmpe)_2(CH_3CN)_2]^{2+}$, $[Co(dmpe)_2(CH_3CN)]^+$, *cis*-$[(H)_2Co(dmpe)_2]^+$, and $HCo(dmpe)_2$ are shown in Figure 2, structures A–D, respectively. Metric parameters for each structure are listed in Table 1. The molecular structure of $[Co(dmpe)_2(CH_3CN)_2]^{2+}$ (Figure 2, structure A) crystallized

dx.doi.org/10.1021/ic200857x | *Inorg. Chem.* 2011, 50, 11914–11928

Table 1. Selected Bond Distances (Å) and Angles (deg) for $HCo(dmpe)_2$, *cis*-$[(H)_2Co(dmpe)_2][BF_4]$, $[Co(dmpe)_2(CH_3CN)][BF_4]$, $[Co(dmpe)_2(CH_3CN)_2][BF_4]_2$

$HCo(dmpe)_2$[a]			
Co(2)−P(3)	2.1306(12)	P(3)−Co(2)−P(4)	89.24(5)
Co(2)−P(4)	2.0847(12)	P(3)−Co(2)−P(5)	114.23(5)
Co(2)−P(5)	2.1325(12)	P(3)−Co(2)−P(6)	110.14(4)
Co(2)−P(6)	2.1164(11)	P(4)−Co(2)−P(5)	119.76(5)
Co(2)−H(2M1)	1.62(3)	P(4)−Co(2)−P(6)	132.63(5)
		P(5)−Co(2)−P(6)	91.81(4)
		H(2M1)−Co(2)−P(3)	161.5(15)
		H(2M1)−Co(2)−P(4)	72.8(15)
		H(2M1)−Co(2)−P(5)	79.6(15)
		H(2M1)−Co(2)−P(6)	80.3(15)
cis-$[(H)_2Co(dmpe)_2][BF_4]$			
Co(1)−P(1)	2.198(3)	P(1)−Co(1)−P(2)	91.72(12)
Co(1)−P(2)	2.180(6)	P(1)−Co(1)−P(3)	103.57(7)
Co(1)−P(3)	2.1934(8)	P(1)−Co(1)−P(4)	103.25(17)
Co(1)−P(4)	2.166(6)	P(2)−Co(1)−P(3)	105.84(15)
Co(1)−H(1C)	1.45(3)	P(2)−Co(1)−P(4)	157.0(2)
Co(1)−H(1D)	1.40(3)	P(3)−Co(1)−P(4)	87.79(19)
		P(1)−Co(1)−H(1C)	86.7(11)
		P(2)−Co(1)−H(1C)	80.6(11)
		P(3)−Co(1)−H(1C)	167.5(11)
		P(4)−Co(1)−H(1C)	82.8(11)
		P(1)−Co(1)−H(1D)	168.3(14)
		P(2)−Co(1)−H(1D)	79.9(14)
		P(3)−Co(1)−H(1D)	86.7(13)
		P(4)−Co(1)−H(1D)	82.5(14)
		H(1C)−Co(1)−H(1D)	83.9(16)
$[Co(dmpe)_2(CH_3CN)][BF_4]$			
Co(1)−P(1)	2.1703(5)	P(1)−Co(1)−P(2)	84.78(2)
Co(1)−P(2)	2.1699(5)	P(1)−Co(1)−P(3)	166.13(2)
Co(1)−P(3)	2.1732(5)	P(1)−Co(1)−P(4)	93.60(2)
Co(1)−P(4)	2.1811(5)	P(2)−Co(1)−P(3)	91.90(2)
Co(1)−N(1)	1.9841(16)	P(2)−Co(1)−P(4)	161.68(2)
		P(3)−Co(1)−P(4)	85.32(2)
		N(1)−Co(1)−P(1)	97.75(5)
		N(1)−Co(1)−P(2)	103.36(5)
		N(1)−Co(1)−P(3)	96.12(5)
		N(1)−Co(1)−P(4)	94.94(5)
$[Co(dmpe)_2(CH_3CN)_2][BF_4]_2$			
Co(1)−P(1)	2.2419(9)	P(1)−Co(1)−P(2)	85.54(3)
Co(1)−P(2)	2.2434(9)	P(1)−Co(1)−P(2A)	94.46(3)
Co(1)−N(1)	2.254(3)	P(1)−Co(1)−P(1A)	180.0
Co(2)−P(3)	2.2412(9)	P(1)−Co(1)−N(1)	87.14(8)
Co(2)−P(4)	2.2465(9)	P(3)−Co(2)−P(4)	85.86(3)
Co(2)−N(2)	2.271(3)	P(3)−Co(2)−P(3A)	180.00(4)
		P(3)−Co(2)−P(4A)	94.14(3)
		P(3)−Co(2)−N(2)	89.16(8)

[a]Metric parameters representing one of the three independent molecules in the unit cell; see the Supporting Information for additional bond distances and angles.

with two independent molecules per asymmetric unit. Each molecule exhibits octahedral coordination geometry with nearly identical metric parameters. The complex is composed of two dmpe ligands occupying the equatorial plane and two acetonitrile ligands in the axial coordination sites. The average Co−P bond distance is 2.2433(9) Å, while the Co−N bond distances are similar at 2.254(3) and 2.271(3) Å. The dmpe bite angle is measured at 85.54(3)° and 85.86(3)° for P1−Co(1)−P2 and P3−Co(2)−P4, respectively.

The molecular structure of $[Co(dmpe)_2(CH_3CN)]^+$ (Figure 2, structure B) is square-pyramidal with the dmpe ligands occupying the equatorial plane and acetonitrile bound in the axial site. The Co−P bond distances are shorter than the analogous Co(II) complex with an average bond length of 2.1736(5) Å. The Co−N bond distance is 1.9841(16) Å.

The molecular structure of the cationic dihydride *cis*-$[(H)_2Co(dmpe)_2]^+$ (Figure 2, structure C) is best described as a distorted octahedron. The chelating dmpe ligands are arranged in a *cis* configuration. The average Co−P bond distance is 2.184(6) Å. The hydride ligands, located from the difference map, occupy the two remaining coordination sites and exhibit Co−H bond distances of 1.45(3) and 1.40(3) Å. The Co−P bond distances *trans* to the hydride ligands are slightly longer, 2.198(3) and 2.1934(8) Å, than those *trans* to phosphine ligands, 2.180(6) and 2.166(6) Å. The bond angles of P(1)−Co(1)−P(2) and P(3)−Co(1)−P(4) for the chelating dmpe ligands are 91.72(12)° and 87.79(19)°; however, deviation from ideal octahedral geometry of 180° is more obvious in the P(1)−Co(1)−H(1D) and P(3)−Co(1)−H(1C) bond angles of 168.3(14)° and 167.5(11)°, respectively, and the P(2)−Co(1)−P(4) bond angle of 157.0(2)°.

The molecular structure of the neutral five-coordinate cobalt hydride $HCo(dmpe)_2$ (Figure 2, structure D) exhibits distorted trigonal bipyramidal coordination geometry. This complex crystallized with three independent molecules in the asymmetric unit. In each molecule, the equatorial plane is composed of three phosphorus atoms, while a fourth phosphorus atom and a hydride ligand occupy the axial sites. The average Co−P bond distances for each independent molecule are similar at 2.1002(12), 2.1161(12), and 2.1099(12) Å. The hydride ligands were located from the difference map and were refined with all three cobalt hydride distances made equivalent to one another at 1.62(3) Å. The average bond angle between the axial hydride ligand and the axial phosphorus atom is 160.7°.

Molecular structures from single crystal X-ray diffraction studies performed on $[Co(dedpe)_2(CH_3CN)]^{2+}$, $[Co(dedpe)_2]^+$, *trans*-$[(H)_2Co(dedpe)_2]^+$, and $HCo(dedpe)_2$ are depicted in Figure 3, structures A−D, respectively. Table 2 contains selected metric parameters for these complexes. $[Co(dedpe)_2(CH_3CN)]^{2+}$ (Figure 3, structure A) contains two independent molecules in the unit cell, each molecule having a five-coordinate square-pyramidal geometry. The dedpe ligands are arranged about the cobalt center so that the phosphorus atoms with phenyl substituents from one ligand are *trans* to phenyl groups of the opposing ligand. This arrangement is likely favored to decrease steric interactions between opposing ligands. The average Co−P bond length is 2.2649(5) Å. The Co−P bonds with ethyl substituents on phosphorus are slightly longer than those with phenyl substituents. The average dedpe bite angle (i.e., P(1)−Co(1)−P(2)) is 84.6°.

Crystals of $[Co(dedpe)_2]^+$ (Figure 3, structure B) were grown by ethyl ether diffusion into an acetonitrile solution of the metal complex. Our attempts to obtain X-ray quality crystals of $[Co(dedpe)_2(CH_3CN)][BF_4]$ by this combination of solvents was unsuccessful. Instead, after two weeks, blue crystals of the 16-electron complex $[Co(dedpe)_2][BF_4]$ precipitated out of the yellow-orange solution. The complex exhibits a nearly ideal square-planar geometry with a dedpe ligand arrangement equivalent to the previously described structure. The asymmetric unit contains four independent molecules with an average

dx.doi.org/10.1021/ic200857x | *Inorg. Chem.* 2011, 50, 11914−11928

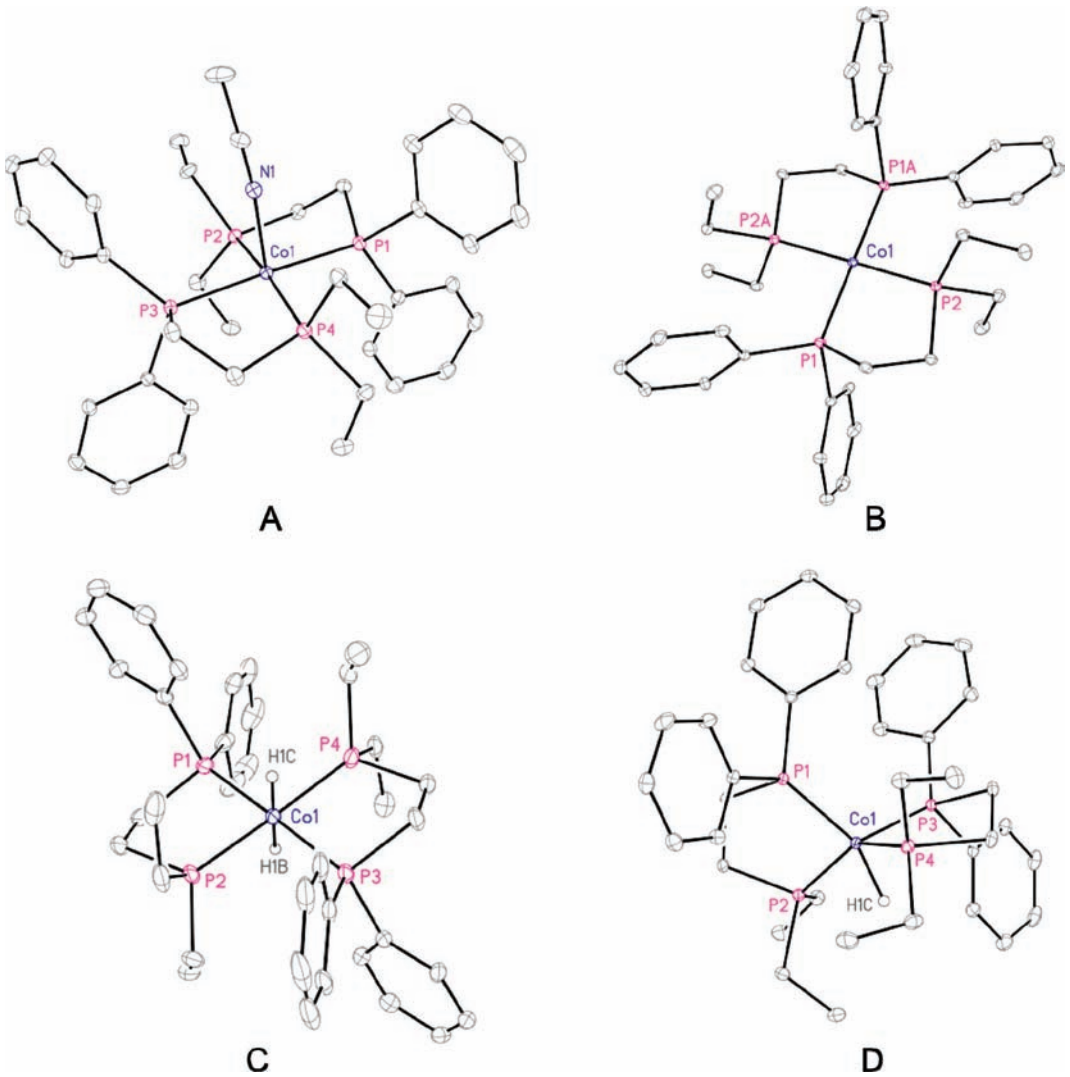

Figure 3. Molecular structures of (A) $[Co(dedpe)_2(CH_3CN)]^{2+}$, (B) $[Co(dedpe)_2]^+$, (C) *trans*-$[(H)_2Co(dedpe)_2]^+$, and (D) $HCo(dedpe)_2$ with atom numbering. Thermal ellipsoids drawn at 30% probability. Hydrogen atoms omitted except for hydride ligands attached to Co in structures C and D.

Co−P bond length of 2.1864(7) Å, shorter than the average Co−P bond length in $[Co(dedpe)_2(CH_3CN)]^{2+}$.

The structure obtained from colorless crystals of *trans*-$[(H)_2Co(dedpe)_2]^+$ (Figure 3, structure C) has nearly ideal octahedral geometry with two dedpe ligands occupying the equatorial plane and the hydride ligands, located from the difference map, positioned in the axial coordination sites in the less commonly observed *trans* stereochemistry.[15,16] The average Co−P bond length is 2.1861(8) Å, similar to other octahedral cobalt(III) cations with chelating diphosphine ligands.[12] The Co−H bond distances were found to be slightly different at 1.40(3) and 1.53(3) Å, and the H(1A)−Co(1)−H(1B) bond angle is nearly linear at 177.9(16)°.

The molecular structure of $HCo(dedpe)_2$ has distorted trigonal-bipyramidal geometry. The equatorial plane consists of phosphorus atoms P3 and P4 from one of the chelating dedpe ligands and P2 of the second chelating dedpe ligand, while the hydride ligand and phosphorus atom P1 of the second dedpe ligand occupy the axial positions. The equatorial Co−P bond lengths are 2.1489(4), 2.1397(5), and 2.1120(4) Å, respectively, while the axial Co−P distance is 2.1357(4) Å. The Co−H bond length is 1.42(2) Å, similar to that of $HCo(dppe)_2$ and $HCo(dppp)_2$.[12,17]

The angles between the hydride ligand and the equatorial phosphorus atoms, namely, P2−Co(1)−H1C and P4−Co(1)−H1C, are acute at 75.3(9)° and 76.6(9)°, while the bond angle in P3−Co(1)−H1C is larger at 90.6(9)°. The P1−Co(1)−H1C bond angle deviates significantly from linearity at 156.3(9)°.

Hydride Donor Abilities of Transition-Metal Hydrides and Hydride Affinities of BX_3 Compounds. The hydride donor abilities of $HCo(dmpe)_2$ and $HCo(dedpe)_2$ were estimated by comparing the difference in hydride donor ability of two systems that have been determined experimentally. Estimates of hydride donor abilities using this approach are a useful tool to check experimentally determined values.[5] For example, the experimentally determined hydride donor abilities of $HCo(dppe)_2$ (49 kcal/mol) and $[HNi(dppe)_2]^+$ (63 kcal/mol; dppe = 1,2-bis(diphenylphosphinoethane)) differ by 14 kcal/mol. A similar difference would be expected between $HCo(dmpe)_2$ and $[HNi(dmpe)_2]^+$. The hydride donor ability of $[HNi(dmpe)_2]^+$ was determined to be 51 kcal/mol. On this basis, we estimate a value of 37 kcal/mol for $\Delta G_{H^-}{}^\circ$ for $HCo(dmpe)_2$. Likewise, using the experimentally

dx.doi.org/10.1021/ic200857x | *Inorg. Chem.* 2011, 50, 11914–11928

Table 2. Selected Bond Distances (Å) and Angles (deg) for $HCo(dedpe)_2$, *trans*-$[(H)_2Co(dedpe)_2][BF_4]$, $[Co(dedpe)_2][BF_4]$, and $[Co(dedpe)_2(CH_3CN)][BF_4]_2$

$HCo(dedpe)_2$			
Co(1)–P(1)	2.1357(4)	P(1)–Co(1)–P(2)	88.387(17)
Co(1)–P(2)	2.1120(4)	P(1)–Co(1)–P(3)	112.374(17)
Co(1)–P(3)	2.1489(4)	P(1)–Co(1)–P(4)	107.613(17)
Co(1)–P(4)	2.1397(5)	P(2)–Co(1)–P(3)	117.100(18)
Co(1)–H(1C)	1.42(2)	P(2)–Co(1)–P(4)	140.121(18)
		P(3)–Co(1)–P(4)	90.808(17)
		H(1C)–Co(1)–P(1)	156.3(9)
		H(1C)–Co(1)–P(2)	75.3(9)
		H(1C)–Co(1)–P(3)	90.6(9)
		H(1C)–Co(1)–P(4)	76.6(9)
trans-$[(H)_2Co(dedpe)_2][BF_4]$			
Co(1)–P(1)	2.1719(8)	P(1)–Co(1)–P(2)	85.85(3)
Co(1)–P(2)	2.1964(9)	P(1)–Co(1)–P(3)	177.64(4)
Co(1)–P(3)	2.1707(8)	P(1)–Co(1)–P(4)	94.34(3)
Co(1)–P(4)	2.1893(8)	P(2)–Co(1)–P(3)	94.05(3)
Co(1)–H(1B)	1.40(3)	P(2)–Co(1)–P(4)	176.87(4)
Co(1)–H(1C)	1.53(3)	P(3)–Co(1)–P(4)	85.89(3)
		H(1B)–Co(1)–P(1)	79.6(13)
		H(1B)–Co(1)–P(2)	92.1(13)
		H(1B)–Co(1)–P(3)	98.2(13)
		H(1B)–Co(1)–P(4)	91.0(13)
		H(1C)–Co(1)–P(1)	99.5(10)
		H(1C)–Co(1)–P(2)	89.7(10)
		H(1C)–Co(1)–P(3)	82.8(10)
		H(1C)–Co(1)–P(4)	87.1(10)
		H(1B)–Co(1)–H(1C)	177.9(16)
$[Co(dedpe)_2][BF_4]$			
Co(1)–P(1)	2.1663(6)	P(1)–Co(1)–P(2)	85.18(2)
Co(1)–P(2)	2.2036(7)	P(1)–Co(1)–P(1A)	179.999(10)
Co(2)–P(3)	2.1676(6)	P(1)–Co(1)–P(2A)	94.82(2)
$[Co(dedpe)_2][BF_4]$			
Co(2)–P(4)	2.2108(7)	P(3)–Co(2)–P(4)	85.27(2)
Co(3)–P(5)	2.1682(7)	P(3)–Co(2)–P(3A)	179.998(9)
Co(3)–P(6)	2.1999(7)	P(3)–Co(2)–P(4A)	94.73(2)
Co(4)–P(7)	2.1709(7)	P(5)–Co(3)–P(6)	94.57(3)
Co(4)–P(8)	2.2045(7)	P(5)–Co(3)–P(5A)	180.0
		P(5)–Co(3)–P(6A)	85.43(3)
		P(7)–Co(4)–P(8)	84.63(3)
		P(7)–Co(4)–P(7A)	179.999(1)
		P(7)–Co(4)–P(8A)	95.37(3)
$[Co(dedpe)_2(CH_3CN)][BF_4]_2$			
Co(1)–P(1)	2.2543(5)	P(1)–Co(1)–P(2)	84.646(18)
Co(1)–P(2)	2.2898(5)	P(1)–Co(1)–P(3)	177.47(2)
Co(1)–P(3)	2.2538(5)	P(1)–Co(1)–P(4)	94.663(19)
Co(1)–P(4)	2.2657(5)	P(2)–Co(1)–P(3)	95.756(19)
Co(1)–N(1)	2.0128(16)	P(2)–Co(1)–P(4)	169.42(2)
Co(2)–P(5)	2.2439(5)	P(3)–Co(1)–P(4)	84.483(18)
Co(2)–P(6)	2.2732(5)	N(1)–Co(1)–P(1)	91.43(5)
Co(2)–P(7)	2.2614(5)	N(1)–Co(1)–P(2)	94.38(5)
Co(2)–P(8)	2.2772(5)	N(1)–Co(1)–P(3)	91.03(5)
Co(2)–N(2)	2.0253(16)	N(1)–Co(1)–P(4)	96.18(5)
		P(5)–Co(2)–P(6)	84.383(18)
		P(5)–Co(2)–P(7)	176.06(2)
		P(5)–Co(2)–P(8)	95.297(19)
		P(6)–Co(2)–P(7)	94.822(19)
		P(6)–Co(2)–P(8)	172.95(2)
		P(7)–Co(2)–P(8)	85.017(18)
		N(2)–Co(2)–P(5)	92.15(5)
		N(2)–Co(2)–P(6)	91.07(5)
		N(2)–Co(2)–P(7)	91.72(5)
		N(2)–Co(2)–P(8)	95.97(5)

measured value of 60 kcal/mol for $[HNi(dedpe)_2]^{7+}$, we predict a hydride donor ability of 46 kcal/mol for $HCo(dedpe)_2$. In addition, the estimated hydride donor ability of 37 kcal/mol for $HCo(dmpe)_2$ is in good agreement with the computationally determined hydricity ($\Delta G_{H^-}°$) of 36.3 kcal/mol for $HCo(dmpe)_2$ from Liu and co-workers.[18]

In the previous study, we predicted hydride affinity (HA) values for selected BX_3 complexes using electronic structure calculations.[5] Table 3 lists the calculated HA values for BX_3 compounds used in this study. We include the HA values for $BH(SPh)_2$ and $BH_2(SPh)$ that are intermediates in the reduction of $B(SPh)_3$. Our previous experimental studies show that $HRh(dmpe)_2$ and $[HBEt_3]^-$ have the same hydride donor abilities. This allows us to relate the hydride donor ability and hydride affinity scales shown in Figure 4. In so doing, we assume (1) that the difference between ΔG and ΔH is approximately constant, dominantly due to the loss of translational entropy of H^-, and (2) that the differences in solvation free energies (ΔG_{solv}) of BHX_3^- and BX_3 are constant. However, we realize that this second assumption may break down because the solvation of ions is more strongly dependent on size than is the solvation of neutrals. Therefore, it needs to be considered when estimating relative acceptor

Table 3. Calculated Hydride Affinity Values of BX_3 Compounds[a]

BX_3 compound	hydride affinity $-\Delta H°$ (kcal/mol)
BEt_3	58.7
$B(OPh)_3$	73.0
BH_3	73.7[b]
$BH_2(SPh)$	78.3
$BH(SPh)_2$	80.8
$B(SPh)_3$	86.6
$B(OC_6F_5)_3$	93.3

[a]From reaction enthalpies for hydride transfer from BH_4^- to BX_3 calculated at the B3LYP/aug-cc-pVTZ//B3LYP/DZVP2 level of theory. [b]CCSD(T)/CBS value.[38]

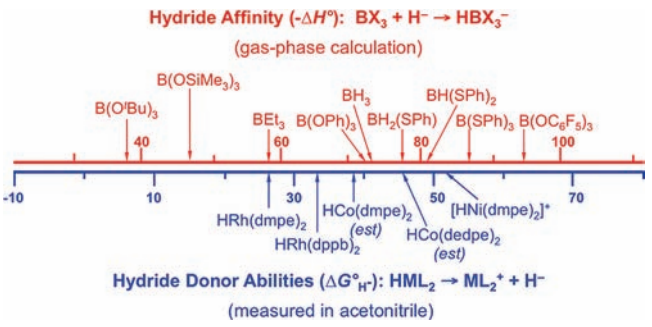

Figure 4. Scales (kcal/mol) of experimentally determined hydride donor abilities of selected transition-metal hydride complexes in acetonitrile (blue, bottom) and the calculated gas-phase hydride affinity values for selected BX_3 compounds (red, top).

dx.doi.org/10.1021/ic200857x | Inorg. Chem. 2011, 50, 11914–11928

abilities. Although Figure 4 is semiquantitative, it was a useful guide in selecting BX_3 compounds to react with the Co and Ni hydrides of this study.

Hydride Transfer from $HCo(dmpe)_2$ to THF-BH_3. Hydride transfer to THF-BH_3 was expected to be thermodynamically close to zero on the basis of our observations in the previous section requiring excess $NaBH_4$ to prepare $HCo(dmpe)_2$, as well as its position in Figure 4. In Figure 4, transition-metal hydrides to the left of a boron complex on the top scale are expected to transfer a hydride from the metal to boron. The addition of 0.5 equiv of THF-BH_3 to a THF solution of $HCo(dmpe)_2$ results in an immediate color change from yellow to orange. The $^{11}B\{^1H\}$ NMR spectrum recorded immediately after mixing, Figure 5, trace A, indicates the

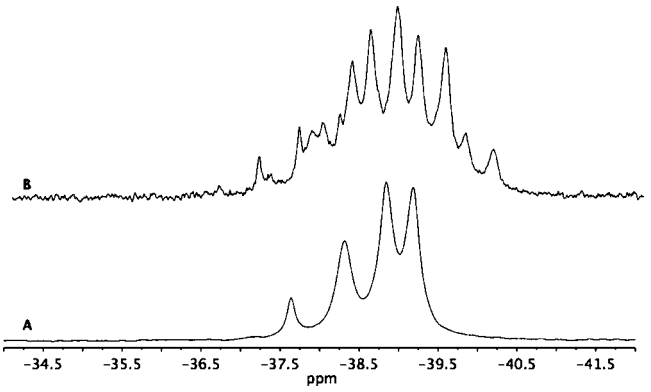

Figure 5. (A) $^{11}B\{^1H\}$ NMR spectrum recorded at 25 °C from the hydride transfer reaction of $HCo(dmpe)_2$ to THF-BH_3. (B) The corresponding ^1H-coupled ^{11}B NMR spectrum.

formation of three new boron-containing products. Indicating that hydride transfer has occurred, a singlet at δ −37.6, a quintet in the ^1H-coupled ^{11}B NMR spectrum, Figure 5, trace B, is assigned as the tetrahydroborate anion of $[Co(dmpe)_2][BH_4]$. The corresponding ^{31}P NMR spectrum contains a singlet at δ 51.8 consistent with $[Co(dmpe)_2]^+$. By comparison, the ^{11}B NMR spectrum of $[Rh(dmpe)_2][BH_4]$, prepared in the hydride transfer reaction between $HRh(dmpe)_2$ and THF-BH_3, appears at δ −37.4.[5] Of the remaining boron-containing products in Figure 5, a doublet centered at δ −39.0 in the $^{11}B\{^1H\}$ NMR spectrum, a doublet of quartets in the ^1H-coupled ^{11}B NMR spectrum, has been identified as dmpe-$(BH_3)_2$, the product of a side reaction where the dmpe ligand has been removed from the cobalt center. The identity of the singlet at δ −38.3, a quintet in the ^1H-coupled ^{11}B NMR spectrum, remains tenuous. The minor variation in chemical shift (δ −37.6 versus −38.3) suggests a slightly different chemical environment or degree of ion pairing for the tetrahydroborate anion than in the discrete complex $[Co(dmpe)_2][BH_4]$. This could be due to the formation of a bridging BH_4^- anion with the cobalt(I) center supported by one or two diphosphines. This type of interaction has been observed in *trans*-$[Fe(H)(dmpe)_2BH_4]$, located at δ −38.1 in the ^{11}B NMR spectrum,[19] and transition metal-tetrahydroborate complexes such as $[(C_6H_5)_3P)_2]Cu(BH_4)$ have been reported.[20] Last, the ^{31}P NMR spectrum after 14 h contained only $HCo(dmpe)_2$ and dmpe-$(BH_3)_2$, while the corresponding ^{11}B NMR indicated dmpe-$(BH_3)_2$ as the only detectible product. This result suggests that the kinetically favored reaction is the hydride transfer to BH_3, while the thermodynamically favored reaction results in the transfer of dmpe from the cobalt center to BH_3.

Hydride Transfer Reactions from Cobalt to BX_3 Complexes: (X = OC_6H_5, OC_6F_5). Experiments also tested the reactivity of $HCo(dmpe)_2$ with $B(OPh)_3$ (HA = 73.0). Because the hydride transfer from $HCo(dmpe)_2$ to THF-BH_3 (HA = 73.7) at room temperature produced $[BH_4]^-$ by ^{11}B NMR spectroscopy, reactions in which a 3-fold excess of $HCo(dmpe)_2$ was mixed with $B(OPh)_3$ were expected to be favorable. We found that $HCo(dmpe)_2$ did not produce hydride transfer products even after refluxing the solution for 12 h. It is notable that, given the nearly identical calculated hydride affinity values for BH_3 and $B(OPh)_3$, hydride transfer was not observed. The difference in reactivity suggests that in cases where the HAs of BX_3 compounds are similar, other factors, such as sterics and solvation free energies of BX_3/BHX_3^-, need to be explicitly considered. In this instance, BH_4^- and $BH(OPh)_3^-$ likely have very different solvation free energies such that the acceptor abilities BH_3 and $B(OPh)_3$ are not as similar as Figure 4 indicates.

In order to increase the hydride acceptor ability of the subject borate ester, electron-withdrawing substituents were incorporated on the aromatic ring. Computational results (Table 3 and Figure 4) indicated that electron-withdrawing groups dramatically increase the hydride acceptor ability of the BX_3 compounds.[5,38] For example, a 3-fold excess of $HCo(dmpe)_2$ reacts with $B(OC_6F_5)_3$, one of the best hydride acceptors, HA = 93 kcal/mol, according to reaction 3. The ^1H-coupled ^{11}B NMR spectrum, Figure 6, trace A, recorded immediately after mixing

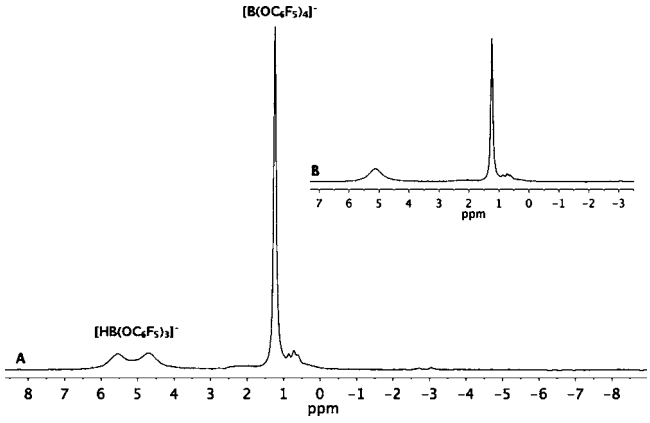

Figure 6. (A) ^1H-coupled ^{11}B NMR spectrum recorded at 25 °C from the hydride transfer reaction of $HCo(dmpe)_2$ to $B(OC_6F_5)_3$. (B) The corresponding $^{11}B\{^1H\}$ NMR spectrum.

indicates the formation of $[HB(OC_6F_5)_3]^-$, a broad doublet at δ 4.9, and $[B(OC_6F_5)_4]^-$, a sharp singlet at δ 1.0.

$$3HCo(dmpe)_2 + B(OC_6F_5)_3 \xrightarrow{THF} [Co(dmpe)_2][HB(OC_6F_5)_3] + [Co(dmpe)_2][B(OC_6F_5)_4] \quad (3)$$

The ^{31}P NMR spectrum contains a sharp singlet at δ 52.9 for $[Co(dmpe)_2]^+$ and a broad resonance at δ 46.4 for unreacted $HCo(dmpe)_2$. Heating the reaction at 50 °C for 6 h produced only a minor increase in the amount of $[HB(OC_6F_5)_3]^-$ by ^{11}B NMR. There were no resonances in the ^{11}B NMR spectra, suggesting the formation of products containing multiple B−H bonds.

Hydride Transfer from $HCo(dmpe)_2$ to $B(SPh)_3$. The hydride transfer reaction between $HCo(dmpe)_2$ and $B(SPh)_3$

dx.doi.org/10.1021/ic200857x | *Inorg. Chem.* 2011, 50, 11914–11928

was anticipated to have a considerable driving force due to the high hydride affinity value of 87 kcal/mol. Additionally, due to a weaker heterolytic B−S bond strength, the formation of multiple B−H bonds was expected in these reactions. For example, in the reaction between a 3-fold excess of HRh-(dmpe)$_2$ with B(SPh)$_3$ in THF, a mixture of products was obtained over the course of the reaction including $[B(SPh)_4]^-$ and $[H_xB(SPh)_{4-x}]^-$ (x = 1−4). When solid B(SPh)$_3$ was added to a THF solution containing a 3-fold excess of HCo(dmpe)$_2$ at room temperature according to reaction 4, the solution color immediately changed from a golden yellow to a red-brown.

$$3HCo(dmpe)_2 + B(SPh)_3 \xrightarrow{THF} \begin{matrix} dmpe{-}(H_2B(SPh))_2 \\ + \\ dmpe{-}(BH_3)_2 \end{matrix} + [H_2B(SPh)_2]^- + Co(dmpe)_2(SPh) \quad (4)$$

The ^{1}H-coupled ^{11}B NMR spectrum Figure 7, trace A, collected immediately after mixing indicated the formation of

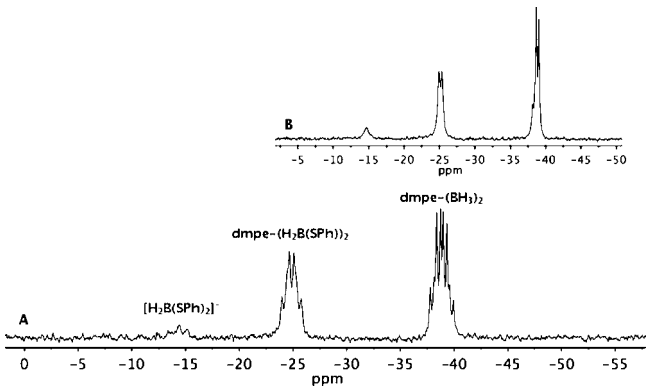

Figure 7. (A) ^{1}H-coupled ^{11}B NMR spectrum from the hydride transfer reaction from HCo(dmpe)$_2$ to B(SPh)$_3$ in THF recorded immediately after mixing. (B) The corresponding ^{11}B{^{1}H} NMR spectrum.

three products containing B−H bonds. A triplet at δ −14.7 was assigned as $[H_2B(SPh)_2]^-$, the result of two hydride transfers to boron. Additionally, multiplets at δ −25.1 and −38.7 are assigned as the phosphine adducts, dmpe-(H$_2$B(SPh))$_2$ and dmpe-(BH$_3$)$_2$, based on the presence of boron−phosphorus coupling of $^1J_{BP}$ = 67 Hz and $^1J_{BP}$ = 56 Hz, respectively, in the ^{11}B{^{1}H} NMR spectrum, Figure 7, trace B. No B(SPh)$_3$ or $[B(SPh)_4]^-$ was observed in the ^{11}B NMR spectrum immediately after mixing. Formation of these B−H containing products indicates that multiple hydride transfers have occurred; however, as observed in the reaction with THF-BH$_3$, decomposition of the cobalt complex resulting from the loss of dmpe ligands is evident. The ^{31}P NMR spectrum shows complete consumption of HCo(dmpe)$_2$ immediately after mixing. The spectrum contains a singlet at δ 44.7 assigned as Co(dmpe)$_2$(SPh) (structurally characterized product isolated from the reaction, Figure S3 in the Supporting Information). Co(dmpe)$_2$(SPh) was prepared independently by the reaction of $[Co(dmpe)_2(CH_3CN)][BF_4]$ with NaSPh in THF to confirm the ^{31}P NMR chemical shift. Also present in the ^{31}P NMR spectrum of the hydride transfer reaction are multiplets corresponding to dmpe-(H$_2$B(SPh))$_2$ and dmpe-(BH$_3$)$_2$ at δ 0.22 and 9.31, respectively. An additional observation from the ^{31}P NMR spectrum was the absence of the signal for $[Co(dmpe)_2]^+$ (singlet at ∼ δ 51) despite the formation of a small amount of the $[H_2B(SPh)_2]^-$ anion. One consideration could be that upon the loss of the dmpe ligands the cobalt cation is stabilized by the formation of a cobalt-THF adduct, $[Co(THF)_x]^+$ (x = 4 or 5). THF adducts such as $[Co(thf)_6]^{2+}$ have been structurally characterized.[21] Efforts to identify this cationic cobalt species product were not pursued.

Hydride transfer between excess HCo(dedpe)$_2$ and B(SPh)$_3$ was surprisingly sluggish. Immediately after mixing, only the starting materials were observed in the ^{31}P and ^{11}B NMR spectra. In fact, no hydride transfer was observed until the reaction was heated at 50 °C for 4 days. After this time, the products noted by ^{11}B NMR included $[B(SPh)_4]^-$ and a small amount of $[HB(SPh)_3]^-$. Decomposition of the cobalt complex was evident due to the presence of a free dedpe ligand in the ^{31}P NMR spectrum. We attribute the limited ability of HCo-(dedpe)$_2$ to transfer the hydride ligand to the steric bulk of the dedpe ligands.

Hydride Transfer from HCo(dmpe)$_2$ to B(SPh)$_3$ in the Presence of NEt$_3$. The results in the previous section demonstrated that hydride transfer from HCo(dmpe)$_2$ to B(SPh)$_3$ led to the formation of products containing multiple B−H bonds. However, during the course of the reaction, an undesirable side reaction occurs where the dmpe ligands of $[Co(dmpe)_2]^+$ are removed from the metal complex and act as a Lewis base to form borane adducts. In an effort to avoid or significantly reduce the decomposition of the cobalt complex, hydride transfer reactions between HCo(dmpe)$_2$ and B(SPh)$_3$ were performed in the presence of triethylamine. The addition of an exogenous donor should provide an alternative Lewis base other than dmpe ligands and drive the reactions toward producing a neutral amine borane product, Et$_3$N-BH$_3$. In a typical reaction, depicted in reaction 5, solid B(SPh)$_3$ was added to a solution of HCo(dmpe)$_2$ in 2 mL of THF and 100 μL of NEt$_3$, resulting in an immediate color change from yellow to orange.

$$3HCo(dmpe)_2 + B(SPh)_3 \xrightarrow[NEt_3]{THF,55°C} Et_3N{-}BH_3 + Et_3N{-}BH_2(SPh) + Co(dmpe)_2(SPh) \quad (5)$$

The ^{1}H-coupled ^{11}B NMR spectrum recorded immediately after mixing, Figure 8, trace A, a singlet at δ 4.2 which indicated the formation of $[B(SPh)_4]^-$ as the major boron-containing product. No B(SPh)$_3$ was observed in the reaction mixture immediately after mixing. In addition, two minor hydride transfer products are observed, a doublet at δ −4.5 and a triplet at δ −6.8, assigned as $[HB(SPh)_3]^-$ and Et$_3$N−H$_2$B(SPh), respectively. The ^{31}P NMR spectrum indicates that HCo-(dmpe)$_2$ and Co(dmpe)$_2$(SPh) are present in roughly equal amounts. Interestingly, there is no evidence for the formation of dmpe-(BH$_3$)$_2$ that had been observed without triethylamine present in the reaction. Heating the reaction for 6 h at 55 °C results in additional formation of B−H bonds and near complete consumption of HCo(dmpe)$_2$ with the concomitant formation of Co(dmpe)$_2$(SPh) by ^{31}P NMR. The ^{1}H-coupled ^{11}B NMR spectrum shown in Figure 8, trace B, contains two borohydride amine adducts: Et$_3$N-BH$_2$(SPh) present as a triplet at δ −6.8 and modest conversion to Et$_3$N-BH$_3$, a quartet

dx.doi.org/10.1021/ic200857x | Inorg. Chem. 2011, 50, 11914−11928

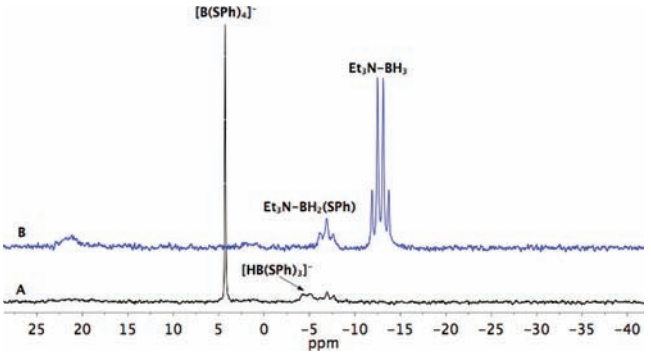

Figure 8. ^{1}H-coupled ^{11}B NMR spectra from the hydride transfer reaction from $HCo(dmpe)_2$ to $B(SPh)_3$ in the presence of NEt_3: (A) Recorded immediately after mixing, (B) recorded after heating for 6 h at 55 °C, showing triethylamineborane, Et_3N-BH_3, at δ −12.8.

centered at δ −12.8, in which case all B−S bonds have been cleaved. Despite initial formation of the four-coordinate thioborate ester, $[B(SPh)_4]^-$, nearly all B−S bonds were cleaved, and multiple B−H bonds were formed with no loss of dmpe ligands from the cobalt complex.

The formation of $Co(dmpe)_2(SPh)$ is prevalent in the hydride transfer reactions noted above. The formation of this product is the result of multiple hydride transfer and ligand redistribution reactions occurring between boron and cobalt, ultimately leading to the thermodynamically favored products, $Co(dmpe)_2(SPh)$ and Et_3N-BH_3. The ligand redistribution reactions are expected to contribute to the driving force for hydride transfer and the formation of B−H bonds. Although a mechanistic study has not been performed, $[Co(dmpe)_2]^+$ clearly participates in assisting with SPh^- redistribution, thus facilitating additional hydride transfer or substituent exchange reactions. A related reaction involving alkali-metal cation participation in a ligand redistribution process was proposed by Nöth and Knizek.[22] Notably, the formation of $Co(dmpe)_2(SPh)$ poses a challenge in the development of a catalytic process, as coordination of SPh^- to cobalt hinders the ability of the metal center to activate H_2.

Hydride Transfer to $B(SPh)_3$ Using $[HNi(dmpe)_2][BPh_4]$ in the Presence of Triethylamine. Thus far, the transition-metal hydride complexes of interest contain chelating diphosphine ligands, e.g., $HM(diphosphine)_2$ complexes where M is Co or Rh. Next, we turned our attention toward transition-metal complexes of the type $[HM'(diphosphine)_2]^+$ where M′ is Ni. The group 10 transition-metal hydride complexes exhibit an overall positive charge, making them less powerful hydride donors compared to the neutral group 9 analogues. As mentioned above, thermochemical data collected for $[HNi(dmpe)_2]^+$ reveal a hydride donor ability of ΔG_{H^-} = 50.7 kcal/mol, and the low cost of nickel compared to Pd or Pt or Rh is an attractive feature in examining the nickel system. Our preliminary reactivity studies focused on reactions between $[HNi(dmpe)_2][BPh_4]$ and $B(SPh)_3$, with the intent of demonstrating that multiple B−H bonds can be formed using transition-metal hydrides that are considerably less hydridic than the Co and Rh analogues.

The reaction of 3 equiv of $[HNi(dmpe)_2][BPh_4]$ with 1 equiv of $B(SPh)_3$ performed in THF in the presence of triethylamine does not immediately form products containing B−H bonds. ^{11}B NMR data recorded immediately after mixing indicates the starting materials $B(SPh)_3$ and $[HNi(dmpe)_2][BPh_4]$ at δ 62.3 and −6.7, respectively, as well as the formation of a small amount of $[B(SPh)_4]^-$ at δ 4.15. The ^{1}H-coupled ^{11}B NMR spectrum recorded after 18 h at 25 °C indicates that a small amount of unreacted $B(SPh)_3$ remained and two B−H containing products were formed. The major product is a triplet corresponding to Et_3N-$BH_2(SPh)$ at δ −7.1, overlapping with $[B(Ph)_4]^-$ at δ −6.7. The minor product is a doublet at δ 4.9, tentatively assigned as Et_3N-$BH(SPh)_2$ (J_{BH} = 130 Hz), a product not previously observed in hydride transfer reactions with cobalt or rhodium where the driving force for hydride transfer is greater than for nickel. After heating the reaction mixture at 50 °C for 24 h, as shown in reaction 6, dark red crystals precipitated from the orange solution. This material was identified as the nickel−thiolate complex $[Ni(dmpe)_2(SPh)][B(Ph)_4]$ (see Figure S4 Supporting Information for X-ray crystal structure).

$$3[HNi(dmpe)_2]^+ + B(SPh)_3 \xrightarrow[NEt_3]{THF,55°C} Et_3N{-}BH_2(SPh) + [Ni(dmpe)_2(SPh)]^+ \quad (6)$$

The ^{11}B NMR of the orange solution indicated that the remaining $B(SPh)_3$ was consumed, and Et_3N-$BH_2(SPh)$ was observed as the only boron containing product, Figure 9, traces

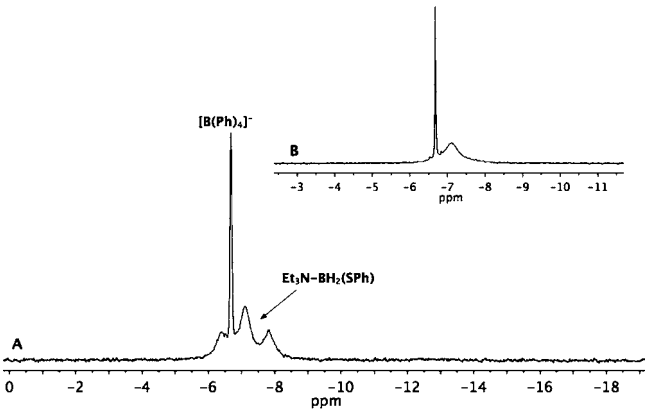

Figure 9. (A) ^{1}H-coupled ^{11}B NMR spectrum from the hydride transfer reaction of $[HNi(dmpe)_2][B(Ph)_4]$ to $B(SPh)_3$ in the presence of triethylamine after heating at 50 °C for 24 h. (B) The corresponding $^{11}B\{^{1}H\}$ NMR spectrum.

A and B. Unlike the reactions with cobalt and rhodium, the completely reduced product, Et_3N-BH_3, was not observed after heating despite the presence of excess $[HNi(dmpe)_2]^+$. The positioned hydride donor ability of $[HNi(dmpe)_2]^+$ (ΔG_{H^-} = 50.7 kcal/mol), relative to the hydride affinity values for $HB(SPh)_2$ and $H_2B(SPh)$ (81 and 78 kcal/mol, respectively) in Figure 4, suggests that hydride transfer should be unfavorable. While $[HNi(dmpe)_2]^+$ appears not to be a strong enough hydride donor to transfer a hydride to $BH_2(SPh)$, we propose the formation of the Ni−S bond in $[Ni(dmpe)_2(SPh)]^+$ and the B−N dative bond in Et_3N-BH_2SPh may offset the unfavorable thermodynamics for hydride transfer to $HB(SPh)_2$, which is a slightly better hydride acceptor than $BH_2(SPh)$. Additionally, the overall positive charge of the complex may contribute to slower reaction rates compared to reactions with cobalt and rhodium hydrides.

dx.doi.org/10.1021/ic200857x | Inorg. Chem. 2011, 50, 11914–11928

SUMMARY AND CONCLUSIONS

This study examines the formation of B−H bonds using nonprecious transition-metal hydrides supported by diphosphine ligands. These five-coordinate transition-metal hydride complexes, $HCo(dmpe)_2$ and $HCo(dedpe)_2$ and $[HNi(dmpe)_2][B(Ph)_4]$, can be prepared from H_2 and a base. On route to the five-coordinate monohydrides, reaction of the cobalt(I) cations, $[Co(dmpe)_2(CH_3CN)]^+$ and $[Co(dedpe)_2(CH_3CN)]^+$, with H_2 affords the six-coordinate dihydride complexes. Structural characterization by X-ray crystallography indicated the formation of *cis*-$[(H)_2Co(dmpe)_2]^+$ and a less commonly observed *trans*-dihydride isomer for *trans*-$[(H)_2Co(dedpe)_2]^+$. The hydride donor abilities of $HCo(dmpe)_2$ and $HCo(dedpe)_2$ were estimated on the basis of comparisons to hydride donor abilities determined experimentally and from computational studies.[18] The hydride donor abilities for the cobalt and nickel systems were cross-referenced to calculated hydride affinities of BX_3 complexes in order to predict when hydride transfer may be favorable. Though the cobalt and nickel hydride complexes exhibit hydride donor abilities significantly less than the previously studied $HRh(dmpe)_2$ system,[5] we observed hydride transfer from $HCo(dmpe)_2$ to BH_3, $B(SPh)_3$, and $B(OC_6F_5)_3$ and from $[HNi(dmpe)_2]^+$ to $B(SPh)_3$. Multiple B−H bonds were formed in the reactions with $B(SPh)_3$, and in the case of Co, the reaction was accompanied by a loss of the dmpe ligands to form dmpe-$(BH_3)_2$. Decomposition was avoided by the addition of triethylamine, which led to the formation of Et_3N-$BH_2(SPh)$ and Et_3N-BH_3 in which nearly all B−S bonds were cleaved. Complete reduction to Et_3N-BH_3 did not occur in reactions of the cationic complex $[HNi(dmpe)_2]^+$ with $B(SPh)_3$. Rather, Et_3N-$BH_2(SPh)$ was the final product. Although hydride transfer from $[HNi(dmpe)_2]^+$ to $HB(SPh)_2$ is predicted to be unfavorable on the basis of the HA of $HB(SPH)_2$, the formation of a Ni−S bond in $[Ni(dmpe)_2(SPh)]^+$ and subsequent formation of Et_3N−H_2B-(SPh) may facilitate hydride transfer. These fundamental hydride transfer studies further our thermodynamic understanding of the factors that govern hydride transfer reactions to BX_3, especially in reactions where there is less driving force for hydride transfer.

EXPERIMENTAL SECTION

Physical Measurements and General Procedures. NMR spectra were recorded in thin-walled quartz NMR tubes (25 °C unless otherwise noted) on a Varian Inova 500 MHz spectrometer equipped with a Sun workstation or a 500 MHz Varian NMR S system. ^{1}H chemical shifts are referenced to residual protons in deuterated solvent. ^{31}P chemical shifts are proton-decoupled unless otherwise noted and referenced to H_3PO_4 as an external reference. ^{11}B chemical shifts are reported relative to BF_3−OEt_2 as an external reference. ^{11}B NMR spectra were integrated to determine the ratio of total boron-containing products in solution. Infrared spectra were recorded on a Nicolet Magna 860 FT-IR spectrometer at ambient temperature and under a purge stream of nitrogen gas. Solid-state FT-IR samples were prepared as KBr pellets. Elemental analysis was performed by Columbia Analytical Services, Tucson, Arizona or Atlantic Microlabs, Norcross, Georgia.

Synthesis and Materials. All synthetic procedures were performed under an atmosphere of N_2 using standard Schlenk or glovebox techniques. Unless described otherwise, all reagents were purchased from commercial sources and were used as received. Solvents were dried by passage through activated alumina in an Innovative Technology, Inc., PureSolv solvent purification system. Deuterated THF was purchased from Cambridge Isotope Laboratories, dried over NaK, and vacuum transferred before use. Triethylamine was purchased from Alfa-Aesar and distilled over CaH_2 before use. Vinyldiphenylphosphine, diethylphosphine, 1,2-bis(dimethylphosphino)-ethane, and Verkade's base ($P(CH_3NCH_2CH_2)_3N$; 2,8,9-trimethyl-2,5,8,9-tetraaza-1-phosphabicyclo[3.3.3]undecane) were purchased from Strem Chemicals, Inc. 2,2′-Azobis(2-methylpropionitrile) (AIBN), borane-THF, ammonium tetraphenylborate, thiophenol, pentafluorophenol, and boron trichloride were purchased from Sigma-Aldrich. High purity grade (99.9%) H_2 gas was passed through a column of Drierite before use. $[Co(CH_3CN)_6][BF_4]_2$[23] was prepared as previously described. $[HNi(dmpe)_2][B(Ph)_4]$ was prepared as previously described[24] substituting $[NH_4][B(Ph)_4]$ for $[NH_4][PF_6]$.

Preparation of dedpe Phosphine Ligand. A reaction flask was charged with 1.2 mL (0.010 mmol) of diethylphosphine, 2.1 mL (0.010 mmol) of vinyldiphenylphosphine, and 0.160 g of 2,2′-azobis(2-methylpropionitrile). The reaction was heated at 70 °C for 2 h. A second portion (0.100 g) of AIBN was added after 2 h, and the reaction was heated at 70 °C for an additional 5 h. Volatile materials were removed under reduced pressure, affording a clear yellow oil. Spectroscopic data matched the previously reported values for dedpe prepared using a Rayonet photoreactor.[7] ^{31}P{^{1}H} NMR (toluene-d_8): δ −12.0 (d, $^3J_{PP}$ = 25 Hz, PPh$_2$), −18.2 (d, $^3J_{PP}$ = 25 Hz, PEt$_2$).

Synthesis of BX_3 Compounds. All aryl borates were synthesized from BCl_3 and the corresponding alcohol or thiol using a low temperature version of the Michaelis method[25] developed by Lappert and co-workers.[26] $B(SPh)_3$ was prepared as previously described.[5]

$HCo(dmpe)_2$, Method A. A solution of Verkade's Base, ($P(CH_3NCH_2CH_2)_3N$; 0.057 g, 0.26 mmol) in 2 mL of THF was added to a stirring solution of *cis*-$[(H)_2Co(dmpe)_2][BF_4]$ (0.121 g, 0.27 mmol) in 10 mL of THF, resulting in a dark yellow solution and the precipitation of a white solid, $[HP(CH_3NCH_2CH_2)_3N][BF_4]$. The solution was stirred for 2 h, filtered through Celite, and the solvent removed under vacuum conditions. The crude solid was extracted with pentane and passed through a plug of APTS-coated silica gel, eluting with pentane. The volatiles were removed under vacuum conditions, affording a bright yellow solid. Yield: 0.050 g, 52%. ^{1}H NMR (THF-d_8): δ 1.47 (s, 8H, PCH_2CH_2), 1.26 (s, 24H, P(CH_3)$_2$), −16.6 (quintet, 1H, Co−H). ^{31}P{^{1}H} NMR (THF-d_8): δ 46.6 (br). IR (KBr): ν_{Co-H} 1856 cm^{-1}. Anal. Calcd for $C_{12}H_{33}CoP_4$: %C, 40.01; % H, 9.23. Found: %C, 40.28; %H, 9.37.

$HCo(dmpe)_2$, Method B. $[Co(dmpe)_2(CH_3CN)_2][BF_4]_2$ (0.461 g, 0.74 mmol) was dissolved in 40 mL of acetonitrile. KC_8 (0.210 g, 1.54 mmol) was added slowly to the stirring solution, resulting in a dark red mixture. After 20 min of stirring, H_2 gas was vigorously bubbled through the solution for 15 min, resulting in a color change to yellow-brown. The mixture was filtered through Celite and the solvent removed under vacuum conditions. The yellow-brown residue was extracted with pentane (∼5−10 mL), filtered through a Celite plug, and concentrated to a volume of 1−2 mL. The dark yellow solution was passed through a plug of APTS-coated silica gel and the yellow product eluted with pentane. The volatiles were removed under vacuum conditions, affording a bright yellow solid. Yield: 0.160 g, 60%.

***cis*-$[(H)_2Co(dmpe)_2][BF_4]$.** KC_8 (0.110 g, 0.81 mmol) was added to a stirring solution of $[Co(dmpe)_2(CH_3CN)_2][BF_4]_2$ (0.455 g, 0.74 mmol) in 40 mL of acetonitrile. Hydrogen gas was vigorously bubbled through the red-brown solution, resulting in a color change to pale yellow. The solution was filtered through Celite and the volatiles removed under vacuum conditions. The remaining solids were dissolved in a minimal amount of THF (∼5 mL) and filtered through Celite. Slow diffusion of ether into the THF solution affords an off-white microcrystalline solid of *cis*-$[(H)_2Co(dmpe)_2][BF_4]$. Yield: 0.156 g, 47%. ^{1}H NMR (THF-d_8): δ 1.96 (s, 8H, PCH_2CH_2), 1.53 (s, 24H, P(CH_3)$_2$), −14.5 (broad singlet, 2H, CoH). ^{31}P{^{1}H} NMR (25 °C) (THF-d_8): δ 61.2 (br), 51.6 (br). IR (KBr): ν_{Co-H} 1877 cm^{-1}. ESI-MS (m/z+, exptl (calcd)): 360.0814 (360.0821). Anal. Calcd for $C_{12}H_{34}CoBF_4P_4$: %C, 32.17; %H, 7.65. Found: %C, 32.43; %H, 7.92.

$[Co(dmpe)_2(CH_3CN)][BF_4]$. Potassium graphite, KC_8 (0.050 g, 0.37 mmol), was slowly added to a stirring solution of $[Co(dmpe)_2(CH_3CN)_2][BF_4]_2$ (0.20 g, 0.35 mmol) in 15 mL of acetonitrile, resulting in a dark red-purple solution. The solution was filtered

dx.doi.org/10.1021/ic200857x | *Inorg. Chem.* 2011, 50, 11914−11928

through Celite to remove graphite and dried under vacuum conditions. The crude solid was extracted with THF and filtered through Celite and dried under vacuum conditions, affording a dark brown solid. Yield: 0.100 g, 64%. ^{1}H NMR (THF-d_8): δ 2.06 (br, 3H, CoNCCH_3), 1.79 (s, 8H, PCH_2CH_2), 1.45 (s, 24H, P(CH_3)$_2$). ^{31}P{^{1}H} NMR (THF-d_8): δ 50.7 (s). IR (KBr): ν_{CN} 2243 cm^{-1}. Anal. Calcd for $C_{14}H_{35}CoBF_4NP_4$: %C, 34.52; %H, 7.24; %N, 2.87. Found: %C, 34.56; %H, 6.76; %N, 1.99.

[Co(dmpe)$_2$(CH$_3$CN)$_2$][BF$_4$]$_2$. A solution of dmpe (1.60 g, 10.6 mmol) in 4 mL of acetonitrile was added to a stirring solution of [Co(CH$_3$CN)$_6$][BF$_4$]$_2$ (2.54 g, 5.3 mmol) in 20 mL of acetonitrile, resulting in a dark red-brown solution. After stirring for 12 h, the solution was filtered through Celite and the solution concentrated (*ca.* 10−12 mL). [Co(dmpe)$_2$(CH$_3$CN)$_2$][BF$_4$]$_2$ was isolated as dark red crystals by diffusing ethyl ether into the acetonitrile solution. The red crystals desolvated and turned pale green over the period of several weeks. The calculated crystalline yield includes two cocrystallized acetonitrile molecules per [Co(dmpe)$_2$(CH$_3$CN)$_2$][BF$_4$]$_2$ as observed by X-ray crystallography. Yield: 3.33 g, 90%. ^{1}H NMR (acetonitrile-d_3): δ −3.6 (br, 24H, P(CH_3)$_2$), −6.7 (br, 8H, PCH_2CH_2). No ^{31}P NMR signal was observed. Anal. Calcd for $C_{14}H_{35}CoB_2F_8NP_4$: %C, 29.30; %H, 6.15; %N, 2.44. Found: %C, 29.34; %H, 6.01; %N, 2.47.

HCo(dedpe)$_2$. KC_8 (0.016 g, 0.12 mmol) was added to a stirring solution of [Co(dedpe)$_2$(CH$_3$CN)][BF$_4$]$_2$ (0.100 g, 0.11 mmol) in 10 mL of acetonitrile resulting in a violet mixture. After stirring for 10 min, the solution was filtered through Celite to remove graphite. Solvent was removed under vacuum conditions, and the brown solids were dissolved in 10 mL of THF. Verkade's base, (P(CH$_3$NCH$_2$CH$_2$)$_3$N; 0.024 g, 0.11 mmol) was added to the THF solution, and H_2 gas was vigorously bubbled through the solution for 2 min, resulting in a slow color change to deep red and the precipitation of [HP(CH$_3$NCH$_2$CH$_2$)$_3$N][BF$_4$]. After stirring for 14 h, the red solution was filtered through Celite, and the solvent was removed under vacuum conditions. The red solids were extracted with pentane (∼5−10 mL), filtered through a Celite plug, concentrated to a volume of 1−2 mL, and passed through a plug of APTS-coated silica gel, eluted with pentane. The red solution was concentrated and stored at −35 °C, affording red crystals after 18 h. Yield: 0.047 g, 63%. ^{1}H NMR (THF-d_8): δ 7.43−6.96 (m, 20H, P(C$_6H_5$)), 2.17 (br, 2H, PCH_2CH_2), 2.02 (br, 2H, PCH_2CH_2), 1.66 (br, 2H, PCH_2CH_2), 1.56 (m, 6H), 1.05 (m, 10H), 0.73 (m, 6H), −15.9 (quintet, $^2J_{PH}$ = 24 Hz, 1H, Co−H). ^{31}P{^{1}H} NMR (THF-d_8): δ 79.1 (s), 74.2 (s). IR (KBr): ν_{Co-H} 1919 cm^{-1}. Anal. Calcd for $C_{36}H_{49}CoP_4$: %C, 65.06; %H, 7.43. Found: %C, 65.39; %H, 7.40.

[(H)$_2$Co(dedpe)$_2$][BF$_4$]. Hydrogen gas was bubbled through an orange solution of [Co(dedpe)$_2$(CH$_3$CN)][BF$_4$] (0.015 g, 0.019 mmol) in 2 mL of acetonitrile for 1 min, resulting in a pale yellow solution and full conversion to the dihydride complex. Removal of the volatiles under vacuum conditions results in a darkening of the material and conversion back to the dark blue [Co(dedpe)$_2$][BF$_4$]. Room temperature ^{1}H and ^{31}P NMR spectra were exceptionally broad and unresolved. ^{1}H NMR (−40 °C; CD$_3$CN): δ 8.03−6.83 (m, P(C$_6H_5$)), 1.96 (s, PCH_2CH_2), 1.53 (s, P(CH_3)$_2$), −10.9 (quintet, *trans*-[(H)$_2$Co(dedpe)$_2$]), −13.6, −14.0, −14.6 (broad multiplets, *cis*-(*H*)$_2$Co). ^{1}H{^{31}P} NMR (−40 °C; CD$_3$CN): −10.9 (br, *trans*-[(*H*)$_2$Co(dedpe)$_2$]), −13.6, −13.7, −14.1, −14.6 (br, *cis*-[(H)$_2$Co(dedpe)$_2$]). ^{31}P NMR (21 °C; CD$_3$CN): δ 89.50 (br), 82.94 (br), 71.50 (br). ^{31}P NMR (−40 °C; CD$_3$CN): δ 95.04 (t, $^2J_{PP}$ = 47 Hz), 92.14 (t, $^2J_{PP}$ = 47 Hz), 90.56 (br), 83.71 (br), 82.25 (br), 75.14 (br), 73.23 (br), 71.36 (br), 67.11 (br).

[Co(dedpe)$_2$(CH$_3$CN)][BF$_4$]. Potassium graphite, KC_8 (0.013 g, 0.096 mmol), was slowly added to a stirring solution of [Co(dedpe)$_2$(CH$_3$CN)][BF$_4$]$_2$ (0.075 g, 0.085 mmol) in 15 mL of acetonitrile, resulting in a dark red-purple solution. The solution was filtered through Celite to remove graphite and dried under vacuum conditions. The crude solid was extracted with THF, filtered through Celite, and dried under vacuum conditions, affording a dark blue solid. Yield: 0.045 g, 70%. ^{1}H NMR (CD$_3$CN): δ 7.67−7.46 (m, 20H, P(C$_6H_5$)), 2.36 (br, 4H, PCH_2CH_2), 1.96 (s, 3H, CoCH_3CN)$_2$), 1.46 (br, 4H, PCH_2CH_2), 1.15 (m, 8H, PCH_2CH$_3$), 0.65 (m, 12H, PCH$_2$CH_3). ^{31}P{^{1}H} NMR (CD$_3$CN): δ 68.8 (t, $^2J_{PP}$ = 63 Hz), 62.8 (br). Anal. Calcd for $C_{36}H_{48}CoBF_4P_4$: %C, 57.62; %H, 6.44. Found: %C, 57.99; %H, 6.33.

[Co(dedpe)$_2$(CH$_3$CN)][BF$_4$]$_2$. A solution of dedpe (1.28 g, 4.2 mmol) in 3 mL of acetonitrile was added to a stirring solution of [Co(CH$_3$CN)$_6$][BF$_4$]$_2$ (1.00 g, 2.1 mmol) in 25 mL of acetonitrile, resulting in a dark red-brown solution. After stirring for 12 h, the solution was filtered through Celite and concentrated to *ca.* 10 mL. [Co(dedpe)$_2$(CH$_3$CN)][BF$_4$]$_2$ was isolated by slowly diffusing ethyl ether into the acetonitrile solution, affording a dark orange microcrystalline solid. Yield: 1.43 g, 78%. ^{1}H NMR (acetonitrile-d_3): δ 10.3 (br, 8H, PCH_2CH_2), 7.2 (br, 20H, P(CH_2CH_3)$_2$), 5.2 (br, 3H, CH_3CN), −1.8 (br, 20H, P(C$_6H_5$)$_2$. No ^{31}P NMR signal was observed. IR (KBr): ν_{CN} 2272 cm^{-1}. Anal. Calcd for $C_{38}H_{51}CoB_2F_8NP_4$: %C, 51.97; %H, 5.85; %N, 1.59. Found: %C, 51.96; %H, 5.85; %N, 1.59.

Reaction of HCo(dmpe)$_2$ with THF-BH$_3$. A total of 20 μL (0.02 mmol) of THF-BH$_3$ (1.0 M solution) was added to a solution of 0.014 g (0.04 mmol) of HCo(dmpe)$_2$ in 1 mL of THF. The tube was shaken to produce an orange-brown solution. The reaction was characterized by ^{11}B and ^{31}P NMR spectroscopy. Spectral data immediately after mixing: ^{11}B{^{1}H}, [^{1}H-coupled] NMR (THF, 25 °C): −37.6 (s, [quintet], $^1J_{BH}$ = 81 Hz, [Co(dmpe)$_2$][BH$_4$], 8%), −38.3 (s, [quintet], $^1J_{BH}$ = 82 Hz, 25%), −39.0 (d, $^1J_{BP}$ = 56 Hz, [dq], $^1J_{BH}$ = 95 Hz dmpe-(BH$_3$)$_2$, 67%). ^{31}P{^{1}H} NMR (THF): δ 51.8 (s, [Co(dmpe)$_2$]$^+$, 14%), 46.4 (s, HCo(dmpe)$_2$, 82%), 8.9 (m, dmpe-(BH$_3$)$_2$, 4%). Spectral data after 14 h at 25 °C: ^{11}B{^{1}H}, [^{1}H-coupled] NMR (THF, 25 °C): −38.8 (d, $^1J_{BP}$ = 55 Hz, [dq], $^1J_{BH}$ = 97 Hz, dmpe-(BH$_3$)$_2$, 100%). ^{31}P{^{1}H} NMR (THF): δ 46.4 (s, HCo(dmpe)$_2$), 8.9 (m, dmpe-(BH$_3$)$_2$).

Reaction of HCo(dmpe)$_2$ with B(OC$_6$F$_5$)$_3$. In a typical experiment, solid B(OC$_6$F$_5$)$_3$ was added to a stirring solution of HCo(dmpe)$_2$ (0.030 mmol) in 2 mL of THF. The reaction was monitored by ^{11}B and ^{31}P NMR spectroscopy. Spectral data immediately after mixing with (0.011 mmol) B(OC$_6$F$_5$)$_3$: ^{11}B{^{1}H}, [^{1}H-coupled] NMR (THF, 50 °C): δ 4.9 (s, [d], $^1J_{BH}$ = 137 Hz, [HB(OC$_6$F$_5$)$_3$]$^-$, 37%), 1.0 (s, [s], [B(OC$_6$F$_5$)$_4$]$^-$, 63%). ^{31}P{^{1}H} NMR (THF): δ 52.9 (s, [Co(dmpe)$_2$]$^+$, 10%), 46.4 (br, HCo(dmpe)$_2$, 88%), −14.7 (s, unassigned, 2%). Spectral data after heating at 50 °C for 6 h: ^{11}B{^{1}H}, [^{1}H-coupled] NMR (THF, 50 °C): δ 4.9 (s, [d], $^1J_{BH}$ = 137 Hz, [HB(OC$_6$F$_5$)$_3$]$^-$, 31%), 1.0 (s, [s], [B(OC$_6$F$_5$)$_4$]$^-$, 61%), 0.62 (d, [d], unassigned, 8%). ^{31}P{^{1}H} NMR (THF): δ 52.9 (s, [Co(dmpe)$_2$]$^+$, 30%), 46.4 (br, HCo(dmpe)$_2$, 67%), −14.7 (s, unassigned, 3%).

Reaction of HCo(dmpe)$_2$ with B(SPh)$_3$. In an NMR tube, 0.0030 g (0.008 mmol) of solid B(SPh)$_3$ was added to 0.014 g (0.04 mmol) of HCo(dmpe)$_2$ in 1.5 mL of THF. The tube was shaken to produce a dark orange solution. The reaction was immediately monitored by ^{11}B and ^{31}P NMR spectroscopy. Spectral data immediately after mixing: ^{11}B{^{1}H}, [^{1}H-coupled] NMR (THF, 25 °C): δ −14.7 (s, [t], $^1J_{BH}$ = 115 Hz, [H$_2$B(SPh)$_2$]$^-$, 6%), −25.1 (d, $^1J_{BP}$ = 67 Hz, [doublet of triplets], $^1J_{BH}$ = 103 Hz, dmpe-(H$_2$B-(SPh))$_2$, 40%), −38.7 (dd, $^1J_{BP}$ = 56 Hz, [dq], $^1J_{BH}$ = 97 Hz, dmpe-(BH$_3$)$_2$, 54%). ^{31}P{^{1}H} NMR (THF): δ 44.7 (s, Co(dmpe)$_2$(SPh), 9.31 (m, dmpe-(BH$_3$)$_2$), 0.22 (m, dmpe-(H$_2$B(SPh))$_2$).

Reaction of HCo(dmpe)$_2$ with B(SPh)$_3$ in the Presence of NEt$_3$. A total of 100 μL (0.72 mmol) of NEt$_3$ was added to 0.014 g (0.038 mmol) of HCo(dmpe)$_2$ in 2 mL of THF, and 0.0035 g (0.010 mmol) of solid B(SPh)$_3$ was added to this mixture. The tube was shaken, and the reaction mixture began to gradually turn orange. The reaction was immediately monitored by ^{11}B and ^{31}P NMR spectroscopy, then again after being heated at 55 °C for 6 h. Spectral data recorded immediately after mixing: ^{11}B{^{1}H}, [^{1}H-coupled] NMR (THF, 25 °C): δ 4.2 (s, [s], [B(SPh)$_4$]$^-$, 65%), −4.5 (s, [d], J_{B-H} = 130 Hz, [HB(SPh)$_3$]$^-$, 19%), −6.8 (s, [t], $^1J_{BH}$ = 120 Hz, Et$_3$N-BH$_2$(SPh), 16%). ^{31}P{^{1}H} NMR (THF): δ 46.5 (br, HCo(dmpe)$_2$, 53%), 44.8 (s, Co(dmpe)$_2$(SPh), 47%). Spectral data after heating 6 h at 55 °C: ^{11}B{^{1}H}, [^{1}H-coupled] NMR (THF, 25 °C): δ 21.3 (br, [br], B−N oligomer, 13%), −6.8 (s, [t], $^1J_{BH}$ = 120 Hz, Et$_3$N-BH$_2$(SPh), 16%), −12.8 (s, [q], $^1J_{BH}$ = 98 Hz, Et$_3$N-BH$_3$, 70%). ^{31}P{^{1}H} NMR (THF): δ 46.5 (br, HCo(dmpe)$_2$, 3%), 44.8 (s, Co(dmpe)$_2$(SPh), 97%).

dx.doi.org/10.1021/ic200857x | *Inorg. Chem.* 2011, 50, 11914−11928

Table 4. Crystallographic Data for $HCo(dmpe)_2$, *cis*-$[(H)_2Co(dmpe)_2][BF_4]$, $[Co(dmpe)_2(CH_3CN)][BF_4]$, and $[Co(dmpe)_2(CH_3CN)_2][BF_4]_2$

	$HCo(dmpe)_2$	*cis*-$[(H)_2Co(dmpe)_2]$ $[BF_4]$	$[Co(dmpe)_2(CH_3CN)]$ $[BF_4]$	$[Co(dmpe)_2(CH_3CN)_2]$ $[BF_4]_2$
empirical formula	$C_{30}H_{82.5}Co_{2.5}P_{10}$	$C_{12}H_{34}BCoF_4P_4$	$C_{14}H_{35}BCoF_4NP_4$	$C_{20}H_{44}B_2CoF_8N_4P_4$
fw	360.19	448.01	487.05	697.02
color, habit	yellow, plates	colorless, blocks	orange, blocks	red, blocks
cryst syst	monoclinic	monoclinic	monoclinic	triclinic
space group	*C*2/*c*	*P*2(1)/*n*	*P*2(1)/*c*	$P\bar{1}$
a, Å	41.817(2)	9.2170(10)	12.4445(3)	8.4911(5)
b, Å	22.9904(11)	19.204(2)	9.1456(2)	12.9468(8)
c, Å	9.7774(5)	12.2850(14)	20.0098(4)	15.0180(9)
α, deg	90	90	90	91.137(4)
β, deg	95.631(2)	97.625(5)	97.5820(10)	92.512(4)
γ, deg	90	90	90	97.786(4)
V (Å^3)	9354.6(8)	2155.2(4)	2257.45(9)	1633.62(17)
λ, Å (Cu (Mo), K*α*)	(0.71073)	(0.71073)	1.54178	1.54178
Z	8	4	4	2
density (g/cm^3)	1.279	1.381	1.433	1.417
temperature (K)	100(2)	135(2)	100(2)	100(2)
2*θ* range, deg	2.59−34.42	1.98−33.26	3.58−68.16	4.48−68.10
μ(Cu (Mo), K*α*), mm^{-1}	(1.242)	(1.118)	8.932	6.551
R(*F*), *Rw*(*F*)[a]	0.0508, 0.1110	0.0471, 0.1081	0.0295, 0.0802	0.0562, 0.1421

[a]Quantity minimized = $R(wF^2) = \sum[w(F_o^2 - F_c^2)^2]/\sum[(wF_o^2)^2]^{1/2}$; $R = \sum\Delta/\sum(F_o)$, $\Delta = |(F_o - F_c)|$, $w = 1/[\sigma^2(F_o^2) + (aP)^2 + bP]$, $P = [2F_c^2 + \mathrm{Max}(F_o,0)]/3$.

Reaction of $[HNi(dmpe)_2][B(Ph)_4]$ with $B(SPh)_3$ in the Presence of NEt_3. $B(SPh)_3$, 0.0040 g (0.012 mmol), was added to a solution of $[HNi(dmpe)_2][B(Ph)_4]$, 0.021 g (0.031 mmol), in 0.6 mL of 5% (v/v) triethylamine in THF, slowly producing an orange solution. Heating the solution resulted in a red solution and the precipitation of dark red crystals of $[Ni(dmpe)_2(SPh)][B(Ph)_4]$. The ratio of products determined by integration of the ^{11}B NMR spectra was difficult due to overlap of the $[B(Ph)_4]^-$ anion with $Et_3N\text{-}BH_2(SPh)$. Spectral data immediately after mixing: $^{11}B\{^1H\}$, [^1H-coupled] NMR (THF, 25 °C): *δ* 62.1 (s, [s], $B(SPh)_3$), −6.7 (s, [s], $[B(Ph)_4]^-$). $^{31}P\{^1H\}$ NMR (THF, 25 °C): *δ* 32.3 (s, $[Ni(dmpe)_2(SPh)]^+$, 1%), 25.7 (s, $[HNi(dmpe)_2]^+$, 99%). Spectral data after 18 h at 25 °C: $^{11}B\{^1H\}$, [^1H-coupled] NMR (THF, 25 °C): *δ* 62.1 (s, [s], $B(SPh)_3$), 4.6 (s, [d], $^1J_{BH}$ = 135 Hz, $Et_3N\text{-}BH(SPh)_2$), −7.1 (s, [t], $^1J_{BH}$ = 117 Hz, $Et_3N\text{-}BH_2(SPh)$), −12.4 (m, unassigned, trace amt). $^{31}P\{^1H\}$ NMR (THF, 25 °C): *δ* 32.3 (s, $[Ni(dmpe)_2(SPh)]^+$, 43%), 25.7 (s, $[HNi(dmpe)_2]^+$, 57%). Spectral data after 24 h 50 °C: ^{11}B NMR (THF, 25 °C): *δ* −7.1 (s, [t], $^1J_{BH}$ = 117 Hz, $Et_3N\text{-}BH_2(SPh)$). $^{31}P\{^1H\}$ NMR (THF, 25 °C): *δ* 32.3 (s, $[Ni(dmpe)_2(SPh)]^+$, 69%), 25.7 (s, $[HNi(dmpe)_2]^+$, 31%). Anal. Calcd for $[Ni(dmpe)_2(SPh)][B(Ph)_4]$, $C_{42}H_{57}BNiP_4S$: %C, 64.07; %H, 7.29. Found: %C, 63.77; %H, 7.32.

X-Ray Diffraction Studies. X-ray diffraction data were collected on a Brüker-AXS Kappa APEX II CCD diffractometer with 0.71073 Å Mo K*α* radiation or 1.54178 Å Cu K*α* radiation. Selected crystals were mounted using Paratone oil onto a glass fiber and cooled to the data collection temperature of 100 K (135 K for *cis*-$[(H)_2Co(dmpe)_2][BF_4]$). For data collection using Mo K*α* radiation unit cell parameters were obtained from 60 data frames, 0.5° Φ, from three different sections of the Ewald sphere. For data collection using Cu K*α* radiation, unit cell parameters were obtained from 90 data frames, 0.5° Φ, from three different sections of the Ewald sphere. Cell parameters were retrieved using APEX II software[27] and refined using SAINT+[28] on all observed reflections. Each data set was treated with SADABS[29] absorption corrections based on redundant multiscan data. The structure was solved by direct methods and refined by least-squares method on F^2 using the SHELXTL program package.[30] Crystallographic data for each structure are listed in Tables 4 and 5. Details regarding specific solution refinement for each compound are provided in the following paragraphs.

$[Co(dmpe)_2(CH_3CN)_2][BF_4]_2\cdot 2CH_3CN$. No symmetry higher than triclinic was evident from the diffraction data. The data set was twinned, and two independent domains were located using *CELL_NOW*.[31] The data set was treated with *TWINABS*[32] absorption corrections based on redundant multiscan data. A solution in the centrosymmetric space group option $P\bar{1}$ yielded chemically reasonable and computationally stable results of refinement. Two independent molecules were located on special positions yielding $Z = 2$ and $Z' = 1$. The asymmetric unit also contains two molecules of acetonitrile located in general positions. The ethyl backbone of one of the chelating dmpe ligands was disordered and subsequently modeled using a second free variable. All non-hydrogen atoms were refined with anisotropic displacement parameters. All hydrogen atoms were treated as idealized contributions. The goodness of fit on F^2 was 1.011 with $R1(wR2) = 0.0537\ (0.1365)$ for $[I\theta > 2(I)]$ and with a largest difference peak and hole of 0.655 and −0.471 e/Å^3.

$[Co(dmpe)_2(CH_3CN)][BF_4]$. The systematic absences in the diffraction data were consistent with the centrosymmetric, monoclinic space group, *P*2(1)/*c*. The asymmetric unit contains one $[Co(dmpe)_2(CH_3CN)]^+$ cation and one $[BF_4]^-$ anion in general positions yielding $Z = 4$ and $Z' = 1$. All non-hydrogen atoms were refined with anisotropic displacement parameters. All hydrogen atoms were treated as idealized contributions. The goodness of fit on F^2 was 1.038 with $R1(wR2) = 0.02957\ (0.0802)$ for $[I\theta > 2(I)]$ and with a largest difference peak and hole of 0.497 and −0.321 e/Å^3.

cis-$[(H)_2Co(dmpe)_2][BF_4]$. The systematic absences in the diffraction data were consistent with the centrosymmetric, monoclinic space group, *P*2(1)/*n*. The molecule was located on a general position yielding $Z = 4$ and $Z' = 1$. All non-hydrogen atoms were refined with anisotropic displacement parameters. The $[(H)_2Co(dmpe)_2]^+$ cation and the $[BF_4]^-$ anion are disordered over two positions. The $[BF_4]^-$ anion positions were located from the difference map and the molecules constrained to be equivalent using DFIX and EADP commands. The $[(H)_2Co(dmpe)_2]^+$ cation showed the chelating phosphines in two different positions which were located from the difference map and allowed to refine freely. The two hydride ligands were located from the difference map and allowed to refine freely. All other hydrogen atoms were treated as idealized contributions. The goodness of fit on F^2 was 1.020 with $R1(wR2) = 0.0471(0.1081)$ for $[I\theta > 2(I)]$ and with a largest difference peak and hole of 0.778 and −0.465 e/Å^3.

dx.doi.org/10.1021/ic200857x | *Inorg. Chem.* 2011, 50, 11914−11928

Table 5. Crystallographic Data for $HCo(dedpe)_2$, *trans*-$[(H)_2Co(dedpe)_2][BF_4]\cdot THF$, $[Co(dedpe)_2][BF_4]$, and $[Co(dedpe)_2(CH_3CN)][BF_4]_2\cdot CH_3CN$

	$HCo(dedpe)_2$	*trans*-$[(H)_2Co(dedpe)_2]$ $[BF_4]\cdot THF$	$[Co(dedpe)_2][BF_4]$	$[Co(dedpe)_2(CH_3CN)]$ $[BF_4]_2\cdot CH_3CN$
empirical formula	$C_{36}H_{49}CoP_4$	$C_{40}H_{58}BOCoF_4OP_4$	$C_{72}H_{96}B_2Co_2F_8P_8$	$C_{78}H_{105}B_4Co_2F_{16}N_3P_8$
fw	664.56	824.48	1500.73	1797.51
color, habit	red, blocks	colorless, blocks	blue, plates	yellow, blocks
cryst syst	orthorhombic	monoclinic	triclinic	monoclinic
space group	*Pbca*	$P2(1)/n$	$P\bar{1}$	$P2(1)/c$
a, Å	18.1830(17)	10.5119(5)	10.4373(13)	22.7320(6)
b, Å	18.9977(17)	25.6399(11)	17.858(2)	19.6783(5)
c, Å	19.7711(18)	14.7044(12)	20.266(3)	19.1975(5)
α, deg	90	90	74.868(6)	90
β, deg	90	91.307(2)	82.200(5)	91.1260(10)
γ, deg	90	90	84.762(5)	90
V(Å^3)	6829.6(11)	3962.2(3)	3606.5(8)	8585.9(4)
λ, Å (Mo, Kα)	0.71073	0.71073	0.71073	0.71073
Z	8	4	2	4
density (g/cm^3)	1.293	1.382	1.382	1.391
temperature (K)	100(2)	100(2)	100(2)	100(2)
2θ range, deg	1.86−33.19	1.60−33.53	1.97−33.48	1.37−33.17
μ(Mo, Kα), mm^{-1}	0.714	0.645	0.699	0.614
$R(F)$, $Rw(F)^a$	0.0399, 0.0839	0.0622, 0.1338	0.0728, 0.1873	0.0453, 0.1004

^{a}Quantity minimized = $R(wF^2) = \sum[w(F_o^2 - F_c^2)^2]/\sum[(wF_o^2)^2]^{1/2}$; $R = \sum\Delta/\sum(F_o)$, $\Delta = |(F_o - F_c)|$, $w = 1/[\sigma^2(F_o^2) + (aP)^2 + bP]$, $P = [2F_c^2 + \mathrm{Max}(F_o,0)]/3$.

$HCo(dmpe)_2$. The systematic absences in the diffraction data were consistent with the centrosymmetric, monoclinic space group, $C2/c$. The asymmetric unit contained three independent molecules with one located on a special position and two on general positions yielding $Z = 8$ and $Z' = 2.5$. All non-hydrogen atoms were refined with anisotropic displacement parameters. The hydrogen atoms were treated as idealized contributions except for the cobalt hydride atoms that were located from the difference map and allowed to refine with all three cobalt hydride distances made equivalent to one another, as would be expected chemically. The three molecules all exhibit disorder in the chelating phosphine ligands over two positions. Modeling of this disorder was successful for two out of the three molecules, with the third being minor and unable to be located from the difference map. The molecule that sits on the special position also has a hydride disordered over two positions about the symmetry element. The goodness of fit on F^2 was 1.025 with $R1(wR2) = 0.0508(0.1110)$ for $[I\theta > 2(I)]$ and with a largest difference peak and hole of 1.674 and −2.364 e/Å^3. The minor residual density is due to the unresolved disorder about the phosphine ligands described above.

$[Co(dedpe)_2(CH_3CN)][BF_4]_2\cdot CH_3CN$. The systematic absences in the diffraction data were consistent with the centrosymmetric, monoclinic space group, $P2(1)/c$. The asymmetric unit contains two $[Co(dedpe)_2(CH_3CN)]^+$ cations, four $[BF_4]^-$ anions, and one acetonitrile molecule yielding $Z = 4$ and $Z' = 2$. Two of the $[BF_4]^-$ anions were disordered over two positions and modeled as such using a second free variable. The acetonitrile molecule was disordered about the nitrogen and was split to eliminate the large thermal parameter. All non-hydrogen atoms were refined with anisotropic displacement parameters. All hydrogen atoms were treated as idealized contributions. The goodness of fit on F^2 was 1.013 with $R1(wR2) = 0.0453(0.1004)$ for $[I\theta > 2(I)]$ and with a largest difference peak and hole of 1.127 and −0.829 e/Å^3.

$[Co(dedpe)_2][BF_4]$. No symmetry higher than triclinic was evident from the diffraction data. Solution in the centrosymmetric space group $P\bar{1}$ yielded chemically reasonable and computationally stable results of refinement. The asymmetric unit contains four $[Co(dedpe)_2]^+$ cations located on special positions and two $[BF_4]^-$ anions located on general positions yielding $Z = 2$ and $Z' = 2$. Two of the four $[Co(dedpe)_2]^+$ cations are disordered about their symmetry elements, leading to two equivalent chelating phosphine positions. The disorder is minimal as determined by free variable refinement and could not be modeled appropriately. This disorder does not change the overall identity of the molecules. All non-hydrogen atoms were refined with anisotropic displacement parameters. Hydrogen atoms were treated as idealized contributions. The goodness of fit on F^2 was 1.024 with $R1(wR2) = 0.0728(0.1873)$ for $[I\theta > 2(I)]$ and with a largest difference peak and hole of 5.213 and −0.621 e/Å^3. The large residual density is due to disorder of the chelating phosphine ligand about a symmetry element described above.

trans-$[(H)_2Co(dedpe)_2][BF_4]\cdot THF$. The systematic absences in the diffraction data were consistent with the centrosymmetric, monoclinic space group, $P2(1)/n$. The asymmetric unit contains one $[(H)_2Co(dedpe)_2]^+$ cation, one $[BF_4]^-$ anion, and one molecule of THF located on general positions yielding $Z = 4$ and $Z' = 1$. Both the THF molecule and the $[BF_4]^-$ anion were disordered over two positions, which were located from the difference map, and refined on their own individual free variable. One ethyl group of the dedpe ligand was disordered over two positions and refined similarly. All non-hydrogen atoms were refined with anisotropic displacement parameters. Hydrogen atoms were treated as idealized contributions except for the hydrogens attached to Co(1), which were located from the difference map and allowed to refine freely. The goodness of fit on F^2 was 1.004 with $R1(wR2) = 0.0622(0.1338)$ for $[I\theta > 2(I)]$ and with a largest difference peak and hole of 0.584 and −0.984 e/Å^3.

$HCo(dedpe)_2$. The systematic absences in the diffraction data were consistent with the centrosymmetric, orthorhombic space group, *Pbca*. The molecule was located on a general position yielding $Z = 8$ and $Z' = 1$. All non-hydrogen atoms were refined with anisotropic displacement parameters. Hydrogen atoms were treated as idealized contributions except for the hydrogen attached to Co(1), which was located from the difference map and allowed to refine freely. The goodness of fit on F^2 was 1.010 with $R1(wR2) = 0.0399(0.0839)$ for $[I\theta > 2(I)]$ and with a largest difference peak and hole of 0.543 and −0.312 e/Å^3.

Computational Methods. Electronic structure calculations using the NWChem suite of programs[33] were performed to determine hydride affinities of BX_3 compounds in Table 3. Minimum energy structures of the boranes and their corresponding borohydrides were optimized using Density Functional Theory,[34] the B3LYP functional,[35] and DZVP2 basis set.[36] Minimum energy geometries were confirmed to be bound states by the absence of imaginary frequencies, and transition states were confirmed by the presence of exactly one

dx.doi.org/10.1021/ic200857x | *Inorg. Chem.* 2011, 50, 11914–11928

imaginary frequency. Enthalpies and free energies at 298 K of optimized structures were calculated from frequency calculations using the harmonic oscillator-rigid-rotor approximation with entropies corrected for rotational symmetry number.[37] HAs of BX_3 were determined from the calculated enthalpy for the isodesmic metathesis reaction 7 with BH_4^- and HA = 73.7 kcal/mol for BH_3.[38]

$$BX_3 + BH_4^- \rightarrow HBX_3^- + BH_3 \quad (7)$$

$$HA(BX_3) = -\Delta H_1^\circ + 73.7\ \text{kcal/mol} \quad (8)$$

Here, we used single point energies calculated with the aug-cc-pVTZ basis set[39] and the DZVP2 optimized geometries and associated thermal corrections. We deemed this protocol satisfactory on the basis of the following results. Grant et al.[38a] calculated HA = 70.5 kcal/mol for BF_3 using couple cluster theory. We calculated 79.1 and 75.0 at B3LYP/DZVP2 and B3LYP/6-311+G**[40] levels. Calculations using single point energies at the B3LYP/aug-cc-pVTZ//DZVP2 level give 72.5 kcal/mol.

■ ASSOCIATED CONTENT

Supporting Information

Experimental details and cyclic voltammetry data for $[Co(dmpe)_2(CH_3CN)_2][BF_4]_2$ and $[Co(dedpe)_2(CH_3CN)][BF_4]_2$; full X-ray diffraction refinement data (CIF) for $HCo(dmpe)_2$, *cis*-$[(H)_2Co(dmpe)_2][BF_4]$, $[Co(dmpe)_2(CH_3CN)][BF_4]$, $[Co(dmpe)_2(CH_3CN)_2][BF_4]_2$, $HCo(dedpe)_2$, *trans*-$[(H)_2Co(dedpe)_2][BF_4]\cdot THF$, $[Co(dedpe)_2][BF_4]$, $[Co(dedpe)_2(CH_3CN)][BF_4]_2\cdot CH_3CN$, $Co(dmpe)_2(SPh)\cdot HSPh$, and $[Ni(dmpe)_2(SPh)][B(Ph)_4]$; NMR spectral data for the reaction of $[Co(dedpe)_2(CH_3CN)]^+$ and H_2; calculated electronic energies and coordinates for structures in Table 3 and the complete ref 33. This material is available free of charge via Internet at http://pubs.acs.org.

■ AUTHOR INFORMATION

Corresponding Author

*E-mail: michael.mock@pnnl.gov.

■ ACKNOWLEDGMENTS

This work was supported by the U.S. Department of Energy's (DOE) Office of Energy Efficiency and Renewable Energy, Center of Excellence for Chemical Hydrogen Storage. M.J.O. was supported as part of the Center for Molecular Electrocatalysis, an Energy Frontier Research Center funded by the U.S. Department of Energy, Office of Basic Energy Sciences, under FWP 56073. This research was performed in part using the Molecular Science Computing Facility in the William R. Wiley Environmental Molecular Sciences Laboratory, a U.S. Department of Energy (DOE) national scientific user facility located at the Pacific Northwest National Laboratory. The Pacific Northwest National Laboratory is operated by Battelle for DOE. The authors wish to thank Charles Campana for his assistance with the structural solution for $HCo(dmpe)_2$.

■ REFERENCES

(1) (a) Kubas, G. J. *Chem. Rev.* **2007**, *107*, 4152. (b) Heinekey, D. M.; Oldham, W. J. *Chem. Rev.* **1993**, *93*, 913. (c) Jessop, P. G.; Morris, R. H. *Coord. Chem. Rev.* **1992**, *121*, 155.

(2) DuBois, D. L.; Blake, D. M.; Miedaner, A.; Curtis, C. J.; DuBois, M. R.; Franz, J. A.; Linehan, J. C. *Organometallics* **2006**, *25*, 4414.

(3) (a) Marder, T. B. *Angew. Chem., Int. Ed.* **2007**, *46*, 8116. (b) Stephens, F. H.; Pons, V.; Baker, T. R. *J. Chem. Soc., Dalton. Trans.* **2007**, *25*, 2613.

(4) (a) Ramachandran, P. V.; Gagare, P. D. *Inorg. Chem.* **2007**, *46*, 7810. (b) Hausdorf, S.; Baitalow, F.; Wolf, G.; Mertens, F. O. R. L. *Int. J. Hydrogen Energy* **2008**, *33*, 608. (c) Davis, B. L.; Dixon, D. A.; Garner, E. B.; Gordon, J. C.; Matus, M. H.; Scott, B.; Stephens, F. H. *Angew. Chem., Int. Ed.* **2009**, *48*, 6812. (d) Hamilton, C. W.; Baker, R. T.; Staubitz, A.; Manners, I. *Chem. Soc. Rev.* **2009**, *38*, 279. (e) Sutton, A. D.; Burrell, A. K.; Dixon, D. A.; Garner, E. B.; Gordon, J. C.; Nakagawa, T.; Ott, K. C.; Robinson, J. P.; Vasiliu, M. *Science* **2011**, *331*, 1426.

(5) Mock, M. T.; Potter, R. G.; Camaioni, D. M.; Li, J.; Dougherty, W. G.; Kassel, W. S.; Twamley, B.; DuBois, D. L. *J. Am. Chem. Soc.* **2009**, *131*, 14454.

(6) (a) Berning, D. E.; Noll, B. C.; DuBois, D. L. *J. Am. Chem. Soc.* **1999**, *121*, 11432. (b) Curtis, C. J.; Miedaner, A.; Ellis, W. W.; DuBois, D. L. *J. Am. Chem. Soc.* **2002**, *124*, 1918.

(7) Berning, D. E.; Miedaner, A.; Curtis, C. J.; Noll, B. C.; DuBois, M. R.; DuBois, D. L. *Organometallics* **2001**, *20*, 1832.

(8) Raebiger, J. W.; Miedaner, A.; Curtis, C. J.; Miller, S. M.; DuBois, D. L. *J. Am. Chem. Soc.* **2004**, *126*, 5502.

(9) Curtis, C. J.; Miedaner, A.; Raebiger, J. W.; DuBois, D. L. *Organometallics* **2004**, *23*, 511.

(10) (a) Price, A. J.; Ciancanelli, R.; Noll, B. C.; Curtis, C. J.; DuBois, D. L.; DuBois, M. R. *Organometallics* **2002**, *21*, 4833. (b) Miedaner, A.; Raebiger, J. W.; Curtis, C. J.; Miller, S. M.; DuBois, D. L. *Organometallics* **2004**, *23*, 2670.

(11) Camaioni, D. M.; Heldebrant, D. J.; Linehan, J. C.; Shaw, W. J.; Li, J.; DuBois, D. L.; Autrey, T. *Prepr. Pap.-Am. Chem. Soc., Div. Fuel Chem.* **2007**, *52*, 509.

(12) Ciancanelli, R.; Noll, B. C.; DuBois, D. L.; Rakowski DuBois, M. *J. Am. Chem. Soc.* **2002**, *124*, 2984.

(13) Schunn, R. A. *Inorg. Chem.* **1970**, *9*, 2567.

(14) Kisanga, P. B.; Verkade, J. G.; Schwesinger, R. *J. Org. Chem.* **2000**, *65*, 5431.

(15) Rossin, A.; Caporali, M.; Gonsalvi, L.; Guerri, A.; Lledos, A.; Peruzzini, M.; Zanobini, F. *Eur. J. Inorg. Chem.* **2009**, 3055.

(16) (a) Findlater, M.; Bernskoetter, W. H.; Brookhart, M. *J. Am. Chem. Soc.* **2010**, *132*, 4534. (b) Rybtchinski, B.; Ben-David, Y.; Milstein, D. *Organometallics* **1997**, *16*, 3786. (c) Guggenberger, L. J. *Inorg. Chem.* **1973**, *12*, 1317.

(17) Holah, D. G.; Hughes, A. N.; Maciaszek, S.; Magnuson, V. R.; Parker, K. O. *Inorg. Chem.* **1985**, *24*, 3956.

(18) Qi, X.-J.; Fu, Y.; Liu, L.; Guo, Q.-X. *Organometallics* **2007**, *26*, 4197.

(19) (a) Baker, M. V.; Field, L. D. *J. Chem. Soc., Chem. Commun.* **1984**, 996. (b) Bau, R.; Yuan, H. S. H.; Baker, M. V.; Field, L. D. *Inorg. Chim. Acta* **1986**, *114*, L27. (c) Baker, M. V.; Field, L. D. *Appl. Organomet. Chem.* **1990**, *4*, 543.

(20) Lippard, S. J.; Melmed, K. M. *J. Am. Chem. Soc.* **1967**, *89*, 3929.

(21) Schneider, J. J.; Goddard, R.; Kruger, C. *Z. Naturforsch., B: Chem. Sci.* **1995**, *50*, 448.

(22) Knizek, J.; Nöth, H. *J. Organomet. Chem.* **2000**, *614*−*615*, 168.

(23) Heintz, R. A.; Smith, J. A.; Szalay, P. S.; Weisgerber, A.; Dunbar, K. R.; Beck, K.; Coucouvanis, D. *Inorg. Synth.* **2002**, *33*, 75.

(24) Miedaner, A.; DuBois, D. L.; Curtis, C. J. *Organometallics* **1993**, *12*, 299.

(25) Michaelis, A.; Hillringhaus, F. A. *Ann.* **1901**, *315*, 41.

(26) (a) Colclough, T.; Gerrard, W.; Lappert, M. F. *J. Chem. Soc.* **1955**, 907. (b) Colclough, T.; Gerrard, W.; Lappert, M. F. *J. Chem. Soc.* **1956**, 3006.

(27) *APEX II*, v. 2009.3; Bruker AXS: Madison, WI, 2009.

(28) *SAINT+*, v. 7.56A; Bruker AXS: Madison, WI, 2009.

(29) *SADABS*, v. 2008/1; Bruker AXS Inc.: Madison, WI, 2008.

(30) Sheldrick, G. M. *SHELXTL*, v. 2008; Bruker AXS Inc.: Madison, WI, 2008.

(31) *CELL_NOW*, v. 2008/2; Bruker AXS: Madison, WI, 2008.

(32) *TWINABS*, v. 2008/2; Bruker AXS: Madison, WI, 2008.

(33) Bylaska, E. J.; et al. *NWChem*, version 5.1.1; Pacific Northwest National Laboratory: Richland, WA.

(34) (a) Hohenberg, P.; Kohn, W. *Phys. Rev.* **1964**, *136*, B864. (b) Kohn, W.; Sham, L. J. *Phys. Rev.* **1965**, *140*, A1133.

(35) Becke, A. D. *J. Chem. Phys.* **1993**, *98*, 5648.

(36) Godbout, N.; Salahub, D. R.; Andzelm, J.; Wimmer, E. *Can. J. Chem.* **1992**, *70*, 560.
(37) Fernández-Ramos, A.; Ellingson, B.; Meana-Pañeda, R.; Marques, J.; Truhlar, D. *Theor. Chem. Acc.* **2007**, *118*, 813.
(38) (a) Grant, D. J.; Dixon, D. A.; Camaioni, D. M.; Potter, R. G.; Christe, K. O. *Inorg. Chem.* **2009**, *48*, 8811. (b) Workman, D. B.; Squires, R. R. *Inorg. Chem.* **1988**, *27*, 1846.
(39) (a) Dunning, T. H. Jr. *J. Chem. Phys.* **1989**, *90*, 1007. (b) Kendall, R. A.; Dunning, T. H. Jr.; Harrison, R. J. *J. Chem. Phys.* **1992**, *96*, 6796. (c) Woon, D. E.; Dunning, T. H. Jr. *J. Chem. Phys.* **1993**, *98*, 1358.
(40) Schafer, A.; Huber, C.; Ahlrichs, R. *J. Chem. Phys.* **1994**, *100*, 5829.